R E M A R K S

Claim 1-12, 14, 18, 20, 21, 23, 26, 38-46 and 48-51 are pending. No new matter has been added by way of the present amendment. For instance, claim 26 has been amended to clarify that it does not have the same scope as claim 18. Claims 48 and 49 have been amended to reflect that the GFP obtained from the organism is the unsubstituted GFP. Lastly, newly added claim 51 is supported by originally filed claims 18 and 19. Accordingly, no new matter has been added.

In view of the following remarks Applicants respectfully request that the Examiner withdraw all rejections and allow the currently pending claims.

Interview of April 29, 2004

Applicants take this opportunity to thank the Examiner for the courtesies extended in granting the Interview held on April 29, 2004. The Interview was very beneficial to the Applicants.

Issues under 35 U.S.C. 112, § second paragraph

The Examiner has rejected claims 18, 20, 21, 23, 26, 38-46, 48 and 49 under 35 U.S.C. § 112, second paragraph for the reasons

recited at pages 2 and 3 of the outstanding Office Action. Applicants respectfully traverse these rejections.

First, the Examiner asserts that the claims, which recite the limitations of "Green Fluorescent Protein (GFP)" are unclear. For instance, the Examiner asserts that it is unclear as to what emission spectrum and source organism the term GFP is meant to be limited. However, Applicants submit that there are no indefinite issues raised by the term Green Fluorescent Protein (GFP). This is a term well understood in the art. For instance, as understood in the art, GFP need not be isolated from only *A. victoria*, but also other sources. Additionally, the term "Green" with respect to GFP is not limited to the particular emission spectrum of the color green. This is well known in the art.

To supplement the above arguments, Applicants are providing herewith two references for consideration by the Examiner. The references are Tsien, *Annu. Rev. Biochem.*, 67:509-44 (1998) and Zhang *et al.*, *Nat. Rev. Mol. Cell Biol.*, vol. 3 (12), pp. 906-918 (December 2002). Each of these articles explains that GFP exist in a variety of organisms. Further, the references explain that different GFP molecules have emission spectra covering not only the color green, but also yellow, cyan, etc. As such, Applicants submit that the term "Green Fluorescent Protein" is a fully definite term

having a well understood scope and structure. Reconsideration is respectfully requested.

Second, the Examiner has rejected claim 26, citing that it fails to further limit claim 18. Applicants respectfully traverse and submit that claim 26 has been amended to clarify this issue. Reconsideration is respectfully requested.

Third, the Examiner has rejected claims 48 and 49, asserting that it is unclear whether or not the GFP which is obtained from the organism is intended to be the substituted GFP or the GFP from which the variant protein is made. Applicants submit that the GFP obtained from the organism is the unsubstituted GFP. It is this GFP which is then altered to arrive at the presently claimed nucleic acid. Reconsideration is respectfully requested.

Issues under 35 U.S.C. 112, § first paragraph

The Examiner has rejected claims 18, 20, 21, 23, 26, 38-46, 48 and 49 under 35 U.S.C. § 112, first paragraph for the reasons recited at pages 3 and 4 of the outstanding Office Action. Applicants respectfully traverse this rejection.

The Examiner continues to assert that there is insufficient description in the specification to support the genus as claimed. In particular, the Examiner asserts that sufficient description

exists only for the sequences of SEQ ID. No.: 16, 18, 20 and 22. Applicants respectfully disagree with the Examiner.

Applicants submit that the present claims (in particular independent claim 18, and claims 20, 21, 23, 26, 38-46, 48 and 49 which depend thereon) are fully supported by the present specification. One of ordinary skill in the art would fully understand that Applicants were in possession of the subject matter claimed at the time of filing the application. The present claims include nucleic acid molecules which encode a modified GFP. GFP is well characterized in the art. However, Applicants were the first to mutate the amino acid in the position immediately upstream of the chromophore (this amino acid is in a position corresponding to position 64 of the wild-type GFP).

Moreover, as explained above, the structure of GFP is well known in the art. Thus, the requirement for a GFP imparts structure into the claims, which the Examiner cannot ignore. Applicants have defined the location of the mutation as well as the nature of the chromophore. Accordingly, Applicants respectfully submit that the claims fully satisfy the requirements of 35 USC § 112, first paragraph. Reconsideration and withdrawal of this rejection are therefore requested.

Issues under 35 U.S.C. § 102(a)

The Examiner has rejected claims 18, 20, 21, 23, 26, 39, 40, 43-46 and 48 under 35 U.S.C. § 102(a) as being anticipated by Ward et al. (WO 95/21191), hereinafter referred to as Ward '191. Applicants respectfully traverse this rejection.

The present claims require a nucleic acid molecule encoding a GFP in which the amino acid immediately upstream of the chromophore is substituted with an amino acid selected from Leu, Ile, Val, Gly, and Ala. The claims also define the chromophore as one of SerTyrGly, SerHisGly, ThrHisGly and ThrTyrGly. Based upon this claim language alone, there is no anticipation based upon Ward '191.

Ward '191 fails to suggest or disclose the presently claimed substitution at a location corresponding to position 64 of wild-type GFP (the amino acid immediately upstream of the chromophore). A review of Ward '191 reveals that the amino acid located at position 64 of the molecule is Phe. However, it is exactly the amino acid at a location corresponding to this Phe of Ward '191, which in the present invention is one of Leu, Ile, Val, Gly, or Ala (but not Phe). Further, the Examiner has pointed to a location having a sequence of Ile, followed by

ThrHisGly (residues 229-232) in Ward '191. However, this is not the location of a chromophore.

Other discussion of Ward '191 reveals additional distinctions. Ward '191 commences on page 1, line 21 giving an introduction to the field of bioluminescence. To generate light in a cell, a reaction requiring enzymatic energy takes place. The enzyme responsible for this reaction is called luciferase. The substrate of the enzyme is called luciferin. Whereas luciferase is a protein, encoded by a DNA sequence, luciferin is an organic molecule synthesized through a complex set of enzymatic reactions in the cell. Thus, introducing luciferase into another cell may not be sufficient to generate light, as luciferin must also be present. As luciferin is not easily taken up by all cell types (see page 3, lines 25-29), the requirements of the presence of both luciferase and luciferin has limited the use of bioluminescence. Organisms such as *Aequorea victoria* further contain GFP. In the specific case of *Aequorea victoria*, the luciferin molecule, the substrate of the chemical reaction, is called coelenterazine.

The disclosure of Ward '191 (page 8, lines 23-29) relates to the fact that by modifying the GFP molecule (S65Y), the protein referred to as pre-coelenterazine is formed within the native cellular environment spontaneously forms coelenterazine. Now, upon expression of the pre-coelenterazine peptide (the S65Y modified GFP) along with luciferase genes (see page 16, lines 27-29), an organism which exhibits bioluminescence is obtained. That is, the organism emits light in the dark. By way of distinction to the present invention, GFP do not emit light in the dark, rather GFP emits light when excited by light.

In summary, Applicants submit that no anticipation of the rejected claims exists based upon Ward '191. Accordingly, the Examiner is respectfully requested to withdraw this rejection and allow the currently pending claims.

Provisional Obviousness-Type Double Patenting

The Examiner has provisionally rejected claims 1-3, 8, 9, 10, 11, 12, 18, 20, 21, 26 and 38-46 under the judicially created doctrine of obviousness-type double patenting as being obvious over claims 10-15, 28-31 and 33 of copending application number 09/619,310. The Examiner has also included claims 48-50

in this provisional rejection. Applicants respectfully traverse this provisional rejection.

Applicants note that neither the present application nor copending application no. 09/619,310 have been allowed. As such, Applicants draw the Examiner's attention to MPEP §804 I-B wherein it is explained that if the "provisional" double patenting rejection in one application is the only rejection remaining in that application, the Examiner should then withdraw that rejection and permit the application to issue as a patent, thereby converting the "provisional" double patenting rejection, which has presumably been presented in the other application, into an actual double patenting rejection at the time the first application issues as a patent.

Allowable Subject Matter

The Examiner has indicated that claims 4-7, 14 and 50 are objected to as being dependent upon a rejected base claim, but would be allowable if rewritten into independent format, including all of the limitations of the base claim and any intervening claims. Applicants submit that all currently pending claims are allowable. Accordingly, the Examiner is respectfully requested to withdraw all rejections and allow the currently pending claims.

If the Examiner has any questions or comments, please contact Craig A. McRobbie, (Registration No. 42,874) at the offices of Birch, Stewart, Kolasch & Birch, LLP.

If necessary, the Commissioner is hereby authorized in this, concurrent, and future replies, to charge payment or credit any overpayment to Deposit Account No. 02-2448 for any additional fees required under 37 C.F.R. § 1.16 or under 37 C.F.R. § 1.17; particularly, extension of time fees.

Respectfully submitted,

BIRCH, STEWART, KOLASCH & BIRCH, LLP

By _____ #42,874
Leonard R. Svensson, #30,330

P.O. Box 747
Falls Church, VA 22040-0747
(703) 205-8000

LRS/CAM:bmp
3759-0107P

Attachments: (1) Tsien, *Annu. Rev. Biochem.*, 67:509-44 (1998); and
(2) Zhang *et al.*, *Nat. Rev. Mol. Cell Biol.*, vol. 3 (12), pp. 906-918 (December 2002).

Annu. Rev. Biochem. 1998. 67:509–44

THE GREEN FLUORESCENT PROTEIN

Roger Y. Tsien
Howard Hughes Medical Institute; University of California, San Diego; La Jolla, CA 92093-0647

KEY WORDS: *Aequorea*, mutants, chromophore, bioluminescence, GFP

ABSTRACT

In just three years, the green fluorescent protein (GFP) from the jellyfish *Aequorea victoria* has vaulted from obscurity to become one of the most widely studied and exploited proteins in biochemistry and cell biology. Its amazing ability to generate a highly visible, efficiently emitting internal fluorophore is both intrinsically fascinating and tremendously valuable. High-resolution crystal structures of GFP offer unprecedented opportunities to understand and manipulate the relation between protein structure and spectroscopic function. GFP has become well established as a marker of gene expression and protein targeting in intact cells and organisms. Mutagenesis and engineering of GFP into chimeric proteins are opening new vistas in physiological indicators, biosensors, and photochemical memories.

CONTENTS

0066-4154/98/0701-0509$08.00

NATURAL AND SCIENTIFIC HISTORY OF GFP

Discovery and Major Milestones

Green Fluorescent Protein was discovered by Shimomura et al (1) as a companion protein to aequorin, the famous chemiluminescent protein from *Aequorea* jellyfish. In a footnote to their account of aequorin purification, they noted that "a protein giving solutions that look slightly greenish in sunlight through only yellowish under tungsten lights, and exhibiting a very bright, greenish fluorescence in the ultraviolet of a Mineralite, has also been isolated from squeezates." This description of the appearance of GFP solutions is still accurate. The same group (2) soon published the emission spectrum of GFP, which peaked at 508 nm. They noted that the green bioluminescence of living *Aequorea* tissue also peaked near this wavelength, whereas the chemiluminescence of pure aequorin was blue and peaked near 470 nm, which was close to one of the excitation peaks of GFP. Therefore the GFP converted the blue emission of aequorin to the green glow of the intact cells and animals. Morin & Hastings (3) found the same color shift in the related coelenterates *Obelia* (a hydroid) and *Renilla* (a sea pansy) and were the first to suggest radiationless energy transfer as the mechanism for exciting coelenterate GFPs in vivo. Morise et al (4) purified and crystallized GFP, measured its absorbance spectrum and fluorescence quantum yield, and showed that aequorin could efficiently transfer its luminescence energy to GFP when the two were coadsorbed onto a cationic support. Prendergast & Mann (5) obtained the first clear estimate for the

monomer molecular weight. Shimomura (6) proteolyzed denatured GFP, analyzed the peptide that retained visible absorbance, and correctly proposed that the chromophore is a 4-(*p*-hydroxybenzylidene)imidazolidin-5-one attached to the peptide backbone through the 1- and 2-positions of the ring.

Aequorea and *Renilla* GFPs were later shown to have the same chromophore (7); and the pH sensitivity, aggregation tendency (8), and renaturation (9) of *Aequorea* GFP were characterized. But the crucial breakthroughs came with the cloning of the gene by Prasher et al (10) and the demonstrations by Chalfie et al (11) and Inouye & Tsuji (12) that expression of the gene in other organisms creates fluorescence. Therefore the gene contains all the information necessary for the posttranslational synthesis of the chromophore, and no jellyfish-specific enzymes are needed.

Occurrence, Relation to Bioluminescence, and Comparison with Other Fluorescent Proteins

Green fluorescent proteins exist in a variety of coelenterates, both hydrozoa such as *Aequorea*, *Obelia*, and *Phialidium*, and anthozoa such as *Renilla* (3, 13). In this review, GFP refers to the *Aequorea* protein except where another genus name is specifically indicated. These GFPs seem to be partners with chemiluminescent proteins and to control the color of the emission in vivo. Despite interesting speculations, it remains unclear why these coelenterates glow, why green emission should be ecologically so superior to the blue of the primary emitters, and why the animals synthesize a separate GFP rather than mutate the chemiluminescent protein to shift its wavelengths. Other than *Aequorea* GFP, only *Renilla* GFP has been biochemically well characterized (14). Despite the apparent identity of the core chromophore in *Renilla* and *Aequorea* GFP, *Renilla* GFP has a much higher extinction coefficient, resistance to pH-induced conformational changes and denaturation, and tendency to dimerize (7).

Unfortunately, *Aequorea* GFP genes are the only GFP genes that have been cloned. Several other bioluminescent species also have emission-shifting accessory proteins, but so far the chromophores all seem to be external cofactors such as lumazines (15) or flavins (16), which diminish their attractiveness as biotechnological tags and probes. Likewise phycobiliproteins (17) and peridinin-chlorophyll-a protein (18), which are highly fluorescent and attractively long-wavelength accessory pigments in photosynthesis, use tetrapyrrole cofactors as their pigments. Correct insertion of the cofactors into the apoproteins has not been demonstrated in foreign organisms, so these proteins are not ready to compete with *Aequorea* GFP. A variety of marine organisms fluoresce, but the biochemistry of the fluorophores is almost completely unknown. Painstaking research like that undertaken by the pioneers of *Aequorea* and *Renilla* GFP would be needed before cloning efforts could begin. It is unclear

whether any investigators or granting agencies are still patient enough to undertake and fund such long-term groundwork.

PRIMARY, SECONDARY, TERTIARY, AND QUATERNARY STRUCTURE

Primary Sequence from Cloning

The sequence of wild-type *Aequorea* GFP (10) is given in Figure 1. Sequences of at least four other isoforms are known (19), though none of the mutations seem to be in positions known to influence protein behavior. Most cDNA constructs derived from the original sequence contain the innocuous mutation Q80R, probably resulting from a PCR error (11). Also, the gene has been resynthesized with altered codons and improved translational initiation sequences (see section on "Promoters, Codon Usage, and Splicing").

The chromophore is a *p*-hydroxybenzylideneimidazolinone (10, 20) formed from residues 65–67, which are Ser-Tyr-Gly in the native protein. Figure 2 shows the currently accepted mechanism (21–23) for chromophore formation. First, GFP folds into a nearly native conformation, then the imidazolinone is formed by nucleophilic attack of the amide of Gly67 on the carbonyl of residue 65, followed by dehydration. Finally, molecular oxygen dehydrogenates the α-β bond of residue 66 to put its aromatic group into conjugation with the imidazolinone. Only at this stage does the chromophore acquire visible absorbance and fluorescence. This mechanism is based on the following arguments: (*a*) Atmospheric oxygen is required for fluorescence to develop (21, 24). (*b*) Fluorescence of anaerobically preformed GFP develops with a simple exponential time course after air is readmitted (21, 25), which is essentially unaffected by the concentration of the GFP itself or of cellular cofactors. (*c*) Analogous imidazolinones autoxidize spontaneously (26). (*d*) The proposed

Figure 1 GFP sequences. (*Line 1*) The wild-type (WT) *gfp10* gene as originally cloned and sequenced by Prasher et al (10). (*Line 2*) A popular humanized version (EGFP, Clontech Laboratories, Palo Alto, CA) (64) incorporating (*a*) an optimal sequence for translational initiation (66), including insertion of a new codon GTG; (*b*) mutation of Phe64 to Leu to improve folding at 37°C; (*c*) mutation of Ser65 to Thr to promote chromophore ionization; and (*d*) mutation of His231 to Leu, which was probably inadvertent and neutral. (*Line 3*) WT amino acid sequence. (*Lines 4* and *5*) Numbering of amino acids and differences between EGFP and WT. The inserted Val is numbered 1a to maintain correspondence with the WT numbering. Note that constructs derived from the natural *gfp10* cDNA contain an apparently neutral mutation Gln80 → Arg (Q80R) caused by a PCR error that changed the CAG codon to CGG (11). In some genes artificially resynthesized with different codons, this error was corrected (e.g. 63 and Clontech's EGFP) but was left as an arginine codon in other instances (40, 62).

```
'G     AGT AAA GGA GAA GAA CTT TTC ACT GGA GTT GTC CCA ATT CTT GTT GAA TTA GAT GGT   60
'G GTG AGC AAG GGC GAG GAG CTG TTC ACC GGG GTG GTG CCC ATC CTG GTC GAG CTG GAC GGC
:t     Ser Lys Gly Glu Glu Leu Phe Thr Gly Val Val Pro Ile Leu Val Glu Leu Asp Gly
1 Val               5                  10                  15                  20
 (1a)
  GAT GTT AAT GGG CAC AAA TTT TCT GTC AGT GGA GAG GGT GAA GGT GAT GCA ACA TAC GGA 120
  GAC GTA AAC GGC CAC AAG TTC AGC GTG TCC GGC GAG GGC GAG GGC GAT GCC ACC TAC GGC
  Asp Val Asn Gly His Lys Phe Ser Val Ser Gly Glu Gly Glu Gly Asp Ala Thr Tyr Gly
                  25                  30                  35                  40

  AAA CTT ACC CTT AAA TTT ATT TGC ACT ACT GGA AAA CTA CCT GTT CCA TGG CCA ACA CTT 180
  AAG CTG ACC CTG AAG TTC ATC TGC ACC ACC GGC AAG CTG CCC GTG CCC TGG CCC ACC CTC
  Lys Leu Thr Leu Lys Phe Ile Cys Thr Thr Gly Lys Leu Pro Val Pro Trp Pro Thr Leu
                  45                  50                  55                  60

  GTC ACT ACT TTC TCT TAT GGT GTT CAA TGC TTT TCA AGA TAC CCA GAT CAT ATG AAA CAG 240
  GTG ACC ACC CTG ACC TAC GGC GTG CAG TGC TTC AGC CGC TAC CCC GAC CAC ATG AAG CAG
  Val Thr Thr Phe Ser Tyr Gly Val Gln Cys Phe Ser Arg Tyr Pro Asp His Met Lys Gln
            Leu Thr                 70                  75                  80
                  65
  CAT GAC TTT TTC AAG AGT GCC ATG CCC GAA GGT TAT GTA CAG GAA AGA ACT ATA TTT TTC 300
  CAC GAC TTC TTC AAG TCC GCC ATG CCC GAA GGC TAC GTC CAG GAG CGC ACC ATC TTC TTC
  His Asp Phe Phe Lys Ser Ala Met Pro Glu Gly Tyr Val Gln Glu Arg Thr Ile Phe Phe
                  85                  90                  95                  100

  AAA GAT GAC GGG AAC TAC AAG ACA CGT GCT GAA GTC AAG TTT GAA GGT GAT ACC CTT GTT 360
  AAG GAC GAC GGC AAC TAC AAG ACC CGC GCC GAG GTG AAG TTC GAG GGC GAC ACC CTG GTG
  Lys Asp Asp Gly Asn Tyr Lys Thr Arg Ala Glu Val Lys Phe Glu Gly Asp Thr Leu Val
                  105                 110                 115                 120

  AAT AGA ATC GAG TTA AAA GGT ATT GAT TTT AAA GAA GAT GGA AAC ATT CTT GGA CAC AAA 420
  AAC CGC ATC GAG CTG AAG GGC ATC GAC TTC AAG GAG GAC GGC AAC ATC CTG GGG CAC AAG
  Asn Arg Ile Glu Leu Lys Gly Ile Asp Phe Lys Glu Asp Gly Asn Ile Leu Gly His Lys
                  125                 130                 135                 140

  TTG GAA TAC AAC TAT AAC TCA CAC AAT GTA TAC ATC ATG GCA GAC AAA CAA AAG AAT GGA 480
  CTG GAG TAC AAC TAC AAC AGC CAC AAC GTC TAT ATC ATG GCC GAC AAG CAG AAG AAC GGC
  Leu Glu Tyr Asn Tyr Asn Ser His Asn Val Tyr Ile Met Ala Asp Lys Gln Lys Asn Gly
                  145                 150                 155                 160

  ATC AAA GTT AAC TTC AAA ATT AGA CAC AAC ATT GAA GAT GGA AGC GTT CAA CTA GCA GAC 540
  ATC AAG GTG AAC TTC AAG ATC CGC CAC AAC ATC GAG GAC GGC AGC GTG CAG CTC GCC GAC
  Ile Lys Val Asn Phe Lys Ile Arg His Asn Ile Glu Asp Gly Ser Val Gln Leu Ala Asp
                  165                 170                 175                 180

  CAT TAT CAA CAA AAT ACT CCA ATT GGC GAT GGC CCT GTC CTT TTA CCA GAC AAC CAT TAC 600
  CAC TAC CAG CAG AAC ACC CCC ATC GGC GAC GGC CCC GTG CTG CTG CCC GAC AAC CAC TAC
  His Tyr Gln Gln Asn Thr Pro Ile Gly Asp Gly Pro Val Leu Leu Pro Asp Asn His Tyr
                  185                 190                 195                 200

  CTG TCC ACA CAA TCT GCC CTT TCG AAA GAT CCC AAC GAA AAG AGA GAC CAC ATG GTC CTT 660
  CTG AGC ACC CAG TCC GCC CTG AGC AAA GAC CCC AAC GAG AAG CGC GAT CAC ATG GTC CTG
  Leu Ser Thr Gln Ser Ala Leu Ser Lys Asp Pro Asn Glu Lys Arg Asp His Met Val Leu
                  205                 210                 215                 220

  CTT GAG TTT GTA ACA GCT GCT GGG ATT ACA CAT GGC ATG GAT GAA CTA TAC AAA TAA TAA 720
  CTG GAG TTC GTG ACC GCC GCC GGG ATC ACT CTC GGC ATG GAC GAG CTG TAC AAG TAA
  Leu Glu Phe Val Thr Ala Ala Gly Ile Thr His Gly Met Asp Glu Leu Tyr Lys Stop
                  225                 230 Leu             235
```

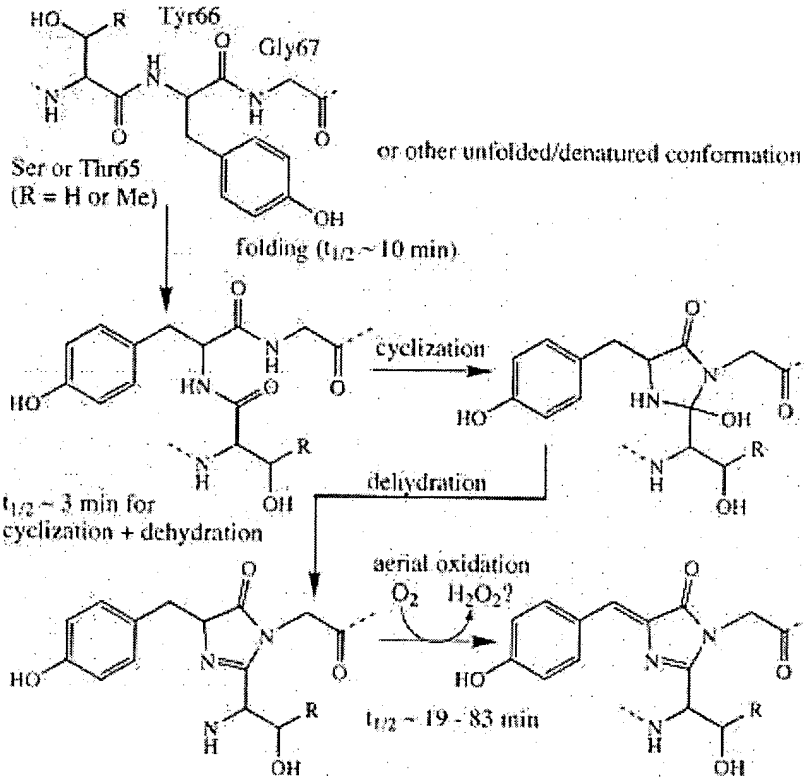

Figure 2 Mechanism proposed by Cubitt et al (22) for the intramolecular biosynthesis of the GFP chromophore, with rate constants estimated for the Ser65 → Thr mutant by Reid & Flynn (23) and Heim et al (25).

cyclization is isosteric with the known tendency for Asn-Gly sequences to cyclize to imides (27). Glycine is by far the best nucleophile in such cyclizations because of its minimal steric hindrance, and Gly67 is conserved in all known mutants of GFP that retain fluorescence. (*e*) Electrospray mass spectra indicate that anaerobically preformed GFP loses only 1 ± 4 Da upon exposure to air, consistent with the predicted loss of two hydrogens (22). This implies that the dehydration (−18 Da) must already have occurred anaerobically and must precede oxidation. (*f*) Reid & Flynn (23) have extensively characterized the kinetics of in vitro refolding of GFP from bacterial inclusion bodies with no chromophore, urea-denatured protein with a mature chromophore, and denatured protein with a chromophore reduced by dithionite. Renaturation was measured by development of fluorescence and resistance to trypsin attack. Their

results support the sequential mechanism and provide the rate constants shown in Figure 2. However, many other aspects of the maturation mechanism remain obscure, such as the steric and catalytic roles of neighboring residues, the means by which mutations can improve folding efficiency, and the dependence of oxidation rate on the oxygen concentration and the protein sequence.

One predicted consequence of oxidation by O_2 is that hydrogen peroxide, H_2O_2, is presumably released in 1:1 stoichiometry with mature GFP. This byproduct might explain occasions when high-level expression of GFP can be deleterious. Perhaps catalase could be useful in such cases. Some difficult GFPs seem to express most readily when targeted to peroxisomes and mitochondria (28; R Rizzuto, T Pozzan, personal communication). Is it a coincidence that these organelles are the best at coping with reactive oxygen species?

Crystal Structures; Tolerance of Truncations

Although GFP was first crystallized in 1974 (4) and diffraction patterns reported in 1988 (29), the structure was first solved in 1996 independently by Ormö et al (30), Protein Data Bank accession number 1EMA, and by Yang et al (31), accession number 1GFL. Both groups relied primarily on multiple anomalous dispersion of selenomethionine groups to obtain phasing information from recombinant protein. Subsequent structures of other crystal forms and mutants (32–34a) have been solved by molecular replacement from the 1EMA coordinates. GFP is an 11-stranded β-barrel threaded by an α-helix running up the axis of the cylinder (Figure 3). The chromophore is attached to the α-helix and is buried almost perfectly in the center of the cylinder, which has been called a β-can (31, 34a). Almost all the primary sequence is used to build the β-barrel and axial helix, so that there are no obvious places where one could design large deletions and reduce the size of the protein by a significant fraction. Residues 1 and 230–238 were too disordered to be resolved; these regions correspond closely to the maximal known amino- and carboxyl-terminal deletions that still permit fluorescence to develop (35). A surprising number of polar groups and structured water molecules are buried adjacent to the chromophore (Figure 4). Particularly important are Gln69, Arg96, His148, Thr203, Ser205, and Glu222.

Dimerization

The excitation spectrum of wild-type GFP changes its shape as a function of protein concentration, implying some form of aggregation (8). The spectroscopic effects of such aggregation are discussed in the section on "Absorbance and Fluorescence Properties." In the Yang et al structure for wild-type GFP (31), the GFP is dimeric. The dimer interface includes hydrophobic residues Ala206, Leu221, and Phe 223 as well as hydrophilic contacts involving Tyr39, Glu142, Asn 144, Ser147, Asn149, Tyr151, Arg168, Asn170, Glu172, Tyr200,

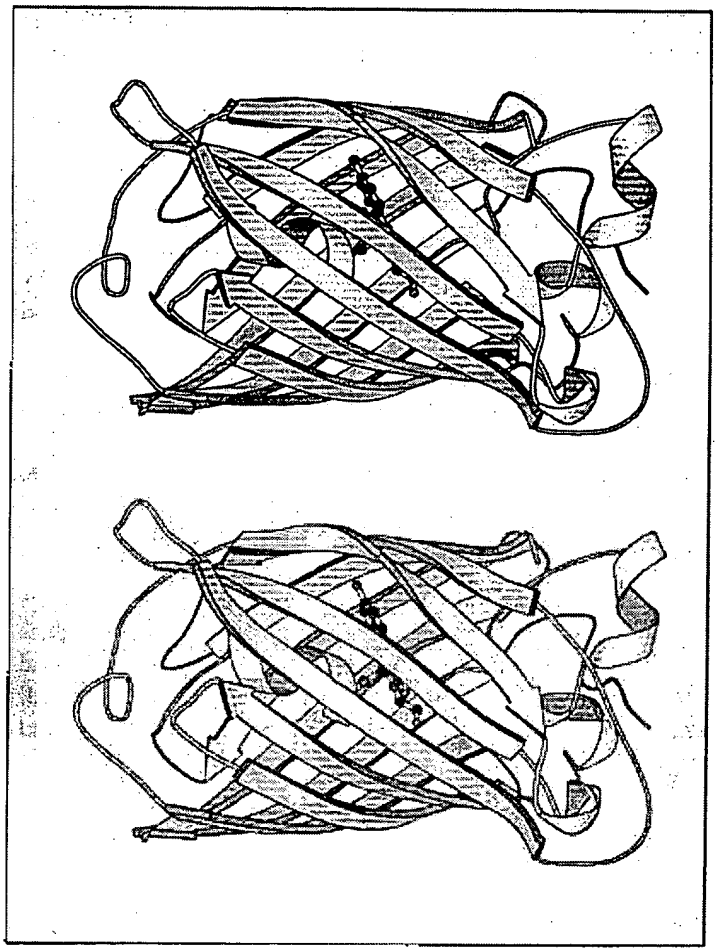

Figure 3 Stereoview of the three-dimensional structure of GFP (30), showing 11 β-strands forming a hollow cylinder through which is threaded a helix bearing the chromophore, shown in ball-and-stick representation. The drawing was prepared by the program MOLSCRIPT and is intended for viewing with uncrossed eyes. Figure courtesy of SJ Remington, University of Oregon.

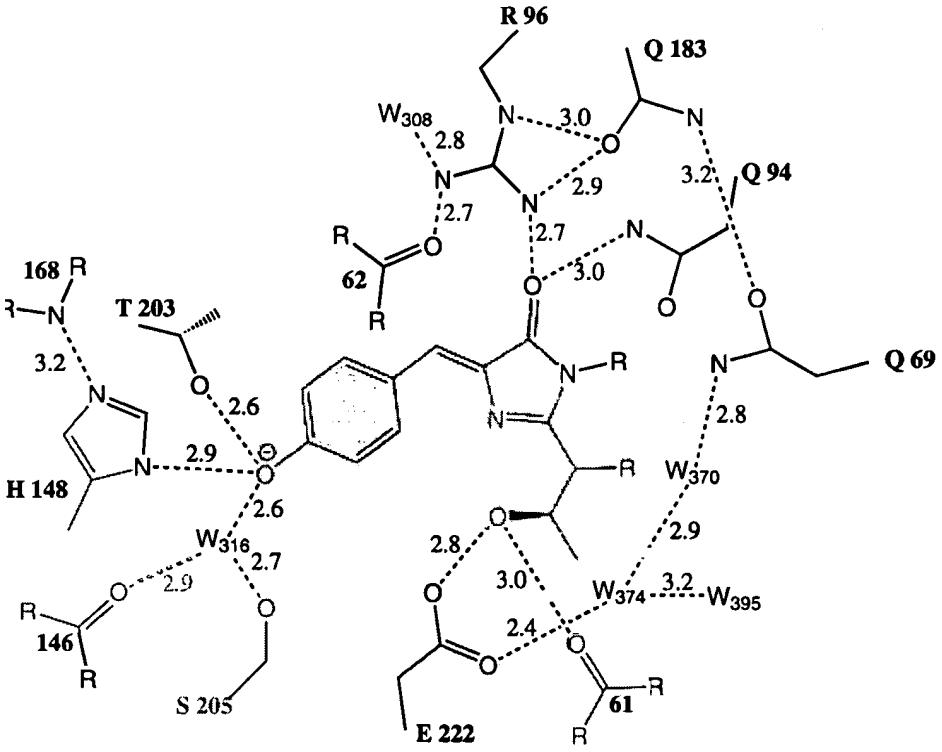

Figure 4 Amino acid side chains, main chain carbonyls and amides, and solvent waters in the immediate vicinity of the chromophore of S65T GFP (30). Side chains are labeled with the one-letter code for the amino acid and the residue number. Main chain groups are labeled with the residue number. Water oxygens are denoted by W and the corresponding serial number within Protein Data Bank structure 1EMA. Probable hydrogen bonds are shown as dotted lines labeled with the distance between the heteroatoms in angstroms. Obviously the true three-dimensional relationships cannot be depicted accurately in this two-dimensional schematic. Figure courtesy of SJ Remington, University of Oregon.

Ser202, Gln204, and Ser208. However, the same wild-type GFP could also crystallize as a monomer (32), isomorphous to the monomeric crystals formed by the S65T mutant (30). Even though GFP can hardly be more concentrated than in a crystal, the formation of dimers seems to be highly dependent on crystal growth conditions rather than an obligatory feature of GFP (33). The dissociation constant for the homodimer has been estimated as 100 μM (34a). By contrast, *Renilla* GFP is an obligate dimer, which is dissociated only under denaturating conditions (14).

ABSORBANCE AND FLUORESCENCE PROPERTIES

Classification of GFPs

The currently known GFP variants may be divided into seven classes based on the distinctive component of their chromophores: class 1, wild-type mixture of neutral phenol and anionic phenolate; class 2, phenolate anion; class 3, neutral phenol; class 4, phenolate anion with stacked π-electron system; class 5, indole; class 6, imidazole; and class 7, phenyl. Each class has a distinct set of excitation and emission wavelengths (Table 1). Classes 1–4 are derived from polypeptides with Tyr at position 66, whereas classes 5–7 result from Trp, His, and Phe at that position. Structures of the resulting chromophores are shown in Figure 5, together with typical fluorescence spectra.

WILD-TYPE MIXTURE OF NEUTRAL PHENOL AND ANIONIC PHENOLATE (CLASS 1)

The wild-type *Aequorea* protein has the most complex spectra of all the GFPs. It has a major excitation peak at 395 nm that is about three times higher in amplitude than a minor peak at 475 nm. In normal solution, excitation at 395 nm gives emission peaking at 508 nm, whereas excitation at 475 nm gives a maximum at 503 nm (21). The fact that the emission maximum depends on the excitation wavelength indicates that the population includes at least two chemically distinct species, which do not fully equilibrate within the lifetime of the excited state. At pH 10–11, when the protein is on the verge of unfolding, increasing pH increases the amplitude of the 475-nm absorbance or excitation peak at the expense of the 395-nm peak (8). The simplest interpretation is that the 475-nm peak arises from GFP molecules containining deprotonated or anionic chromophores, whereas the 395-nm peak represents GFPs containing protonated or neutral chromophores (21, 22). The latter would be expected to deprotonate in the excited state, because phenols almost always become much more acidic in their excited states. Light-induced ionization to the anion would explain why excitation of the neutral chromophores gives emission at greater than 500 nm, similar to but not quite identical to the direct excitation of anionic chromophores. Picosecond spectroscopy gives direct evidence for such excited-state proton transfer (36). After a flash at 395 nm, the emission shifts from a 460- to a 508-nm peak over about 10 ps. These kinetics can be slowed greatly by cooling to 77°K and increasing viscosity, or by deuterium substitution, which argue strongly for excited-state proton transfer.

During most light absorption/emission cycles, the proton transfer eventually reverses. However, occasionally the proton does not return to the chromophore, so the neutral chromophore is photoisomerized to the anionic form. Thus on

Table 1 Spectral characteristics of the major classes of green fluorescent proteins (GFPs)

Mutation[a]	Common name	λ_{exc} (ϵ)[b]	λ_{em} (QY)[c]	Rel. fl.[d] @ 37°C	References[e]
Class 1, wild-type					
None or Q80R	Wild type	395–397 (25–30) 470–475 (9.5–14)	504 (0.79)	6	43, 45
F99S, M153T, V163A	Cycle 3	397 (30) 475 (6.5–8.5)	506 (0.79)	100	43, 45
Class 2, phenolate anion					
S65T		489 (52–58)	509–511 (0.64)	12	43–45
F64L, S65T	EGFP	488 (55–57)	507–509 (0.60)	20	43–45
F64L, S65T, V163A		488 (42)	511 (0.58)	54	44
S65T, S72A, N149K, M153T, I167T	Emerald	487 (57.5)	509 (0.68)	100	44
Class 3, neutral phenol					
S202F, T203I	H9	399 (20)	511 (0.60)	13	44
T203I, S72A, Y145F	H9–40	399 (29)	511 (0.64)	100	44
Class 4, phenolate anion with stacked π-electron system (yellow fluorescent proteins)					
S65G, S72A, T203F		512 (65.5)	522 (0.70)	6	44
S65G, S72A, T203H		508 (48.5)	518 (0.78)	12	44
S65G, V68L, Q69K S72A, T203Y	10C Q69K	516 (62)	529 (0.71)	50	44
S65G, V68L, S72A, T203Y	10C	514 (83.4)	527 (0.61)	58	44
S65G, S72A, K79R, T203Y	Topaz	514 (94.5)	527 (0.60)	100	44
Class 5, indole in chromophore (cyan fluorescent proteins)					
Y66W		436	485	—	21
Y66W, N146I, M153T, V163A	W7	434 (23.9) 452	476 (0.42) 505	61	44
F64L, S65T, Y66W, N146I, M153T, V163A	W1B or ECFP	434 (32.5) 452	476 (0.4) 505	80	44
S65A, Y66W, S72A, N146I, M153T, V163A	W1C	435 (21.2)	495 (0.39)	100	44
Class 6, imidazole in chromophore (blue fluorescent proteins)					
Y66H	BFP	384 (21)	448 (0.24)	18	44
Y66H, Y145F	P4–3	382 (22.3)	446 (0.3)	52	44
F64L, Y66H, Y145F	EBFP	380–383 (26.3–31)	440–447 (0.17–0.26)	100	43, 44
Class 7, phenyl in chromophore					
Y66F		360	442		22

[a]Substitutions from the primary sequence of GFP (see Figure 1) are given as the single-letter code for the amino acid being replaced, its numerical position in the sequence, and the single-letter code for the replacement. Note that many valuable mutants have been left out of this table for reasons of brevity and because quantitative spectral and brightness data were not available; therefore omission does not imply denigration. Phenotypically neutral substitutions such as Q80R, H231L, and insertion of residue 1a (see Figure 1) have also been omitted.

[b]λ_{exc} is the peak of the excitation spectrum in units of nanometers. ϵ in parentheses is the absorbance extinction coefficient in units of $10^3\ M^{-1}\ cm^{-1}$. Estimates of extinction coefficients have tended to increase as expression and purification are optimized; obsolete older values have been omitted. Two numbers separated by a dash indicate a range of estimates from different authors working under slightly different conditions. Two numbers on separate lines indicate two distinct peaks in the excitation spectrum.

[c]λ_{em} is the peak of the emission spectrum in units of nanometers. QY in parentheses is the fluorescence quantum yield, which is dimensionless. The best figure of merit for the overall brightness of properly matured GFPs is the product of ϵ and QY. See footnote b for explanation of pairs of values.

[d]Relative fluorescence intensities for proteins expressed in *Escherichia coli* at 37°C from the same vector background under similar conditions. These numbers include not only the intrinsic brightnesses measured by $\epsilon \cdot$ QY but also the folding efficiencies at 37°C. They are only rough estimates, which will change under different expression conditions. They have been arbitrarily normalized to 100 for the brightest member of each class and cannot be used to compare different classes.

[e]References only for the quantitative spectral and brightness data. References to the origin and use of the mutants have been omitted for lack of space.

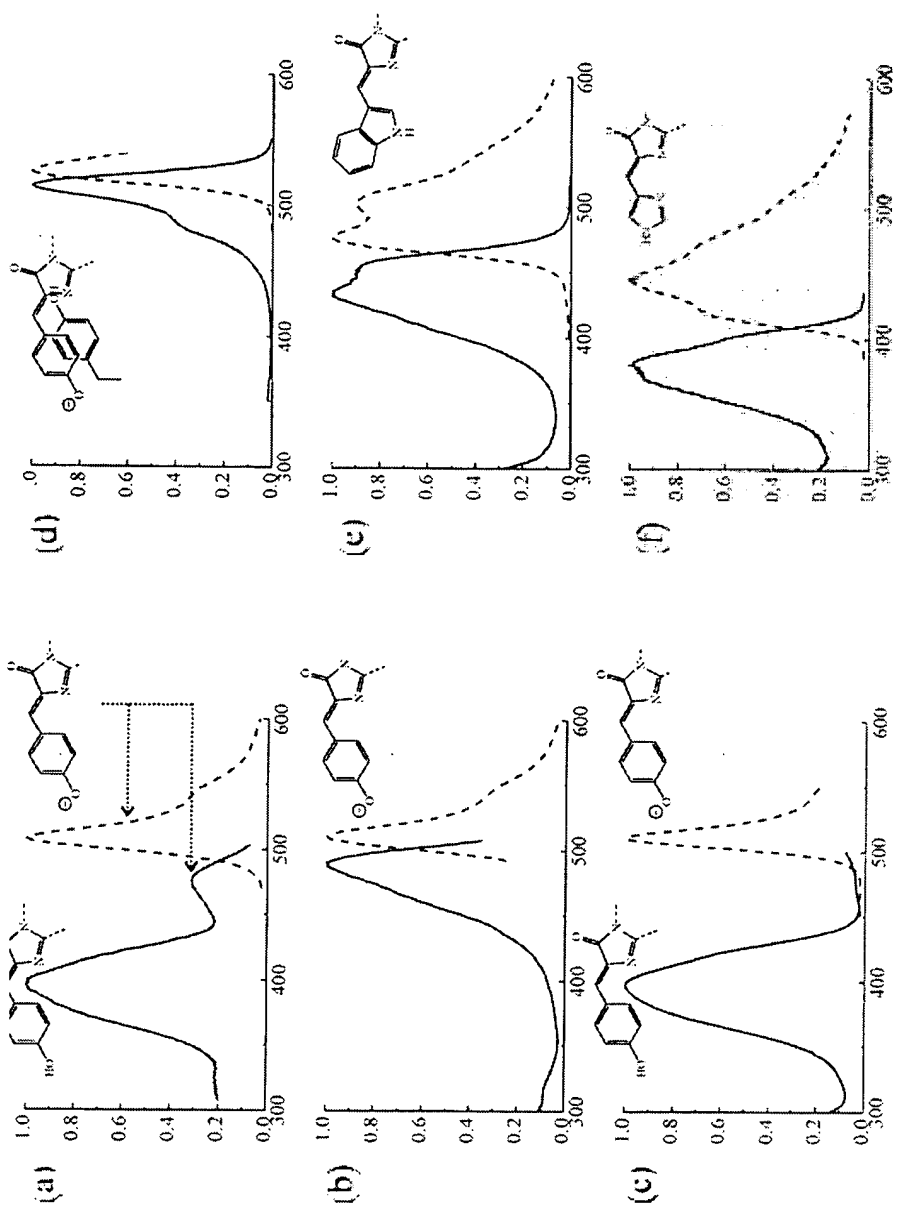
(a)
(b)
(c)
(d)
(e)
(f)
1.0
0.8
0.6
0.4
0.2
0.0
300
400
500
600

intense UV illumination, the 395-nm absorbance and excitation peak of the neutral form gradually declines and the 470-nm peak of the chromophore anion increases (22, 36, 37). Before illumination, wild-type GFP contains about a 6:1 ratio of neutral-to-anionic forms, but with enough UV the percentage of anionic form can increase several-fold. The probable mechanism (32, 33) is that proton transfer occurs via the hydrogen bonds of a buried water and Ser205 to Glu222. Meanwhile the side chain of Thr203 rotates to solvate and stabilize the phenolate oxyanion. In the crystal structure of monomeric wild-type GFP, Thr203 exists in two conformations: approximately 85% with the OH facing away from the phenol oxygen, and 15% with the OH rotated toward it (32). This proportion agrees well with the spectroscopic estimate for the ratio of neutral to anionic chromophores at equilibrium (36).

Wild-type GFP folds fairly efficiently when expressed at or below room temperature, but its folding efficiency declines steeply at higher temperatures. Presumably this natural temperature sensitivity is of no consequence to the jellyfish, which would never encounter warm water in the Pacific Northwest. Temperature sensitivity is restricted to the folding process. GFP that has matured properly at low temperature is stable and fluorescent at temperatures up to at least 65°C. The poor ability of GFP to mature in warm temperatures has been used in pulse-chase experiments in which the fate of fluorescent protein made at low temperatures is followed after restoration of normal warmth and simultaneous suppression of new fluorescence (38, 39). However, for other applications it would be desirable to have a GFP that works well at 37°C.

The most extensive attempt to develop such a mutant while preserving the complex wild-type spectrum utilized DNA shuffling (40), a technique for recombining various mutations while creating new ones. This approach produced a triple mutant, F99S, M153T, V163A, which improved 37°C-folding, reduced aggregation at high concentrations, and increased the diffusibility of the protein inside cells (37). The latter two mutations had already been found by more conventional mutagenesis procedures (41, 42). Such folding mutations do not

Figure 5 Fluorescence excitation and emission spectra (solid and dashed lines, respectively) for typical members of the six major classes of GFP mutants, together with the chromophore structures believed to be responsible for the spectra. Spectra have been normalized to a maximum amplitude of 1. For comparison of absolute brightnesses, see the extinction coefficients and quantum yields in Table 1. When only one structure is drawn, both excitation and emission spectra arise from the same state of chromophore protonation. The actual GFPs depicted are (*a*) wild-type, (*b*) Emerald, (*c*) H9-40, (*d*) Topaz, (*e*) W1B, and (*f*) P4-3. The detailed substitutions within each of these variants are listed in Table 1.

increase the intrinsic brightness of properly matured GFP molecules. Such brightness is measured by the product of extinction coefficient and fluorescence quantum yield (Table 1). The folding mutations merely increase the percentage of molecules that mature properly under adverse conditions, such as 37°C and high GFP concentrations that promote aggregation (33, 43–45). Although the folding mutations are highly valuable and should be incorporated routinely into new constructs, they produce less dramatic or no improvements at lower temperatures and levels of expression. Also the increments in brightness achieved by compounding such mutations will be limited by the obvious fact that folding cannot exceed 100% efficiency.

The coexistence of neutral and anion chromophores giving two excitation peaks in the wild-type spectrum has a few advantages and many disadvantages for cell biological applications. If the GFP fluorescence is to be detected by the naked eye, UV excitation is convenient (40) because UV is inherently invisible. However, because intense UV can damage the eye, an external excitation-blocking filter would be advisable even for visual inspection. Also, scattering, autofluorescence, and the possibility of tissue damage are more severe with UV excitation. Excitation at the 470-nm peak would reduce these problems but is inefficient because only 15% of the protein has the anionic chromophore that absorbs there. The photoisomerization is a major hindrance to quantitation of images, but it also permits the diffusion or trafficking of GFP-labeled proteins to be monitored by locally irradiating a cell with a point or stripe of intense UV and then imaging the subsequent fate of the photoisomerized protein with 470-nm excitation (37).

PHENOLATE ANION IN CHROMOPHORE (CLASS 2) GFPs with phenolate anions in the chromophore have become the most widely used class for routine cell biological use because they were the first group to combine high brightness with simple excitation and emission spectra peaking at wavelengths very similar to fluorescein, the most popular small-molecule fluorophore. The most commonly used mutation to cause ionization of the phenol of the chromophore is a replacement of Ser65 by Thr, or S65T (25), though several other aliphatic residues such as Gly, Ala, Cys, and Leu have roughly similar effects (25, 46, 47). The triple mutation F64M, S65G, Q69L, found by random mutagenesis around the chromophore, has achieved considerable popularity under the name RSGFP4 (46). In both S65T and RSGFP4, the wild-type 395-nm excitation peak due to the neutral phenol is suppressed, and the 470- to 475-nm peak due to the anion is enhanced five- to sixfold in amplitude and shifted to 489–490 nm (25, 46, 48). The oxidation to the mature fluorophore was about fourfold faster in S65T than in the wild type (25). Like wild-type GFP, S65T folds fairly efficiently

when expressed at room temperature or below but tends to misfold and produce mostly nonfluorescent aggregates at higher temperatures. Because of the obvious interest in expression at 37°C, much effort has been devoted to finding additional mutations that give greater brightness at warmer temperatures. The most often used of these have been F64L (47) and V163A (42), though other mutations such as S72A, N149K, M153T, and I167T (33) (Table 1) can also be helpful alone or in combination. As with GFPs of wild-type spectra, such mutations improve only folding efficiency, not the brightness of properly folded molecules.

The probable mechanism by which replacement of Ser65 promotes chromophore ionization (30, 32) is that only Ser65 can donate a hydrogen bond to the buried side chain of Glu222 to allow ionization of that carboxylate, which is within 3.7 Å of the chromophore. Gly, Ala, and Leu cannot donate hydrogen bonds, and Thr and Cys are too large to adopt the correct conformation in the crowded interior of the protein. Such residues at position 65 force the carboxyl of Glu222 to remain neutral. The other polar groups solvating the chromophore are then sufficient to promote its ionization to an anion, whereas if Glu222 is an anion, electrostatic repulsion forbids the chromophore from becoming an anion as well. This hypothesis explains why mutation of Glu222 to Gly gives the same spectral shape and wavelengths (49) as Ser65 mutations. However, practical applications of E222G have not been reported.

NEUTRAL PHENOL IN CHROMOPHORE (CLASS 3) Ionization of the chromophore cannot only be favored but be repressed. Mutation of Thr203 to Ile (21, 49) largely suppresses the 475-nm excitation peak, leaving only the shorter wavelength peak at 399 nm. Presumably a chromophore anion cannot be adequately solvated once the OH of Thr203 is gone, so the chromophore is neutral in almost all the ground-state molecules. However, the emission is still at 511 nm because the excited state remains acidic enough to eject a proton. This mutant and its folding-optimized descendants (Table 1) could be valuable alternatives for UV-excited green fluorescence without the complicated photochemistry of wild-type (class 1) GFPs. Because they lack an excitation maximum near 479–490 nm, they could be used in conjunction with the phenolate anion (class 2) GFPs for double-labeling. Images taken with the two different excitation bands near 400 and 480 nm but the same greater-than-500-nm emission would be compared. Even though the spectral contrast between the two GFPs would not be as great as when both excitation and emission wavelengths are varied, the use of two excitation wavelengths fits the many imaging systems designed for excitation-ratioing indicators and avoids any image registration problems created by alternating emission filters. The neutral phenol GFPs also

have the largest gap in wavelengths between excitation and emission peaks of any of the GFPs. This large Stokes' shift could be advantageous in supporting laser action, where it is important that the dye should have as little absorbance as possible at the wavelengths of fluorescence and lasing.

PHENOLATE ANION WITH STACKED π-ELECTRON SYSTEM (CLASS 4) The longest wavelengths currently available by mutation result from stacking an aromatic ring next to the phenolate anion of the chromophore. So far the aromatic ring has always come from the side chain of residue 203, and residue 65 is Gly or Thr instead of Ser, to promote ionization of the chromophore. All four aromatic residues at that position 203 (His, Trp, Phe, and Tyr) increase the excitation and emission wavelengths by up to 20 nm, with the shifts increasing in the stated order (30). These mutants were rationally designed from the crystal structure of S65T GFP in the expectation that the additional polarizability around the chromophore and π-π interaction would reduce the excited state energy, that is, increase both the excitation and emission wavelengths. The mutants would have been nearly impossible to find by random mutagenesis, because all three bases in the original codon (ACA) encoding Thr203 would have to be replaced to encode an aromatic amino acid, and any random mutation rate high enough to give a significant probability of changing three bases in one codon would mutate so many other residues as to kill the protein.

The actual crystal structure of a mutant containing Tyr203 has verified that its aromatic ring stacks next to the chromophore (RM Wachter, GT Hanson, AB Cubitt, K Kallio, RY Tsien, SJ Remington, manuscript in preparation). Mutation of Gln69 to Lys (Q69K) gives an additional shift of about 1–2 nm, resulting in an emission peak around 529 nm, the longest now known (Table 1). Although 529 nm itself is rather greenish, the tail at longer wavelengths is sufficient to give the fluorescence an overall yellowish appearance, which is clearly distinguishable by eye from the more greenish emission of GFP classes 1–3. Therefore class 4 GFPs have been called YFPs for yellowish fluorescent proteins (50), though this name has also been used for a fluorescent protein from *Vibrio fischeri* (16). The so-called BioYellow variety marketed by Pharmingen (51) is identical to RSGFP4 (46), a class 2 GFP with emission maximum at 505 nm, the same as the wild type.

INDOLE IN CHROMOPHORE DERIVED FROM Y66W (CLASS 5) Substitution of Trp for Tyr66 produces a new chromophore with an indole instead of a phenol or phenolate (21). Excitation and emission wavelengths are 436 and 476 nm, intermediate between neutral phenol and anionic phenolate chromophores. The increased bulk of the indole requires many additional mutations to restore

reasonable brightness (41), but when such mutations are provided, the overall performance is fairly good (Table 1). These proteins are called cyan fluorescent proteins, or CFPs, because of their blue-green or cyan emission. One curious and so far unexplained feature (Figure 5) is that most have double-humped rather than conventional single excitation and emission peaks. The origin of the doubled emission peaks must be vibrational levels or other quantum states that equilibrate within the lifetime of the excited state, because their shapes and relative amplitudes are the same regardless of the excitation wavelength.

IMIDAZOLE IN CHROMOPHORE DERIVED FROM Y66H (CLASS 6) Substitution of His for Tyr 66 puts an imidazole in the chromophore (21) and shifts the wavelengths yet shorter than Trp66. The excitation and emission peaks are around 383 and 447 nm (Table 1), so the emission is blue. A convenient abbreviation is therefore BFP, although other blue fluorescent proteins [e.g. spent aequorin and lumazine-containing proteins from *Photobacterium phosphoreum* (15)] have previously shared the same acronym. Crystal structures for several BFPs have been solved (33, 34). As usual, these proteins benefit considerably from folding mutations (33, 41). BFP and a UV-excitable GFP permit double-labeling of cellular structures with two emission colors arising from a common excitation wavelength near 390 nm (28). However, even with folding improvements BFP still suffers from a relatively low fluorescence quantum yield and relatively easy bleaching (28). A functional dye laser has been constructed with purified BFP as the gain medium, but the duration of lasing at 450 nm is limited by protein bleaching (SJ Remington, D Alavi, M Raymer, RY Tsien, manuscript in preparation).

PHENYL IN CHROMOPHORE DERIVED FROM Y66F (CLASS 7) The very shortest wavelengths are obtained with Phe at 66 (22). This mutant has been little investigated because no obvious practical use for proteins requiring such short wavelength excitation has been proposed. Nevertheless it proves that any aromatic residue at position 66 can form a chromophore.

General Relation of Structure to Spectra

The denatured wild-type protein absorbs maximally at 384 nm at neutral or acidic pH and at 448 nm at alkaline pH, with a pK_a of 8.1 (7). This rough similarity to the absorbance and excitation maxima of the intact protein was a primary motivation for assigning the 395- and 470-nm excitation peaks of the latter to the neutral and anionic chromophores. Denatured GFPs or small proteolytic fragments carrying the chromophore are essentially totally nonfluorescent, presumably because the chromophore is unprotected from quenching by jostling water dipoles, paramagnetic oxygen molecules, or *cis-trans*

isomerization (7, 52). The slight difference in absorbance wavelengths between denatured and intact proteins is not unreasonable for the structured environment of the latter. In particular, Arg96 puts a positively charged guanidinium quite close to the carbonyl group of the imidazolinone. This cation would electrostatically stabilize increased electron-density on the carbonyl oxygen in the chromophore's excited state. This electrostatic attraction would explain much of the red shift of intact protein relative to denatured protein. Indeed, mutation of Arg96 to Cys in S65T blue-shifts the excitation maximum from 489 to 472 nm and the emission maximum from 511 to 503 nm (R Ranganathan, personal communication), supporting a major role for Arg96 in lowering the energy of the excited state. Theoretical calculations of the energy levels of the chromophore in vacuo have led to the proposal that the imidazolinone-ring nitrogen adjacent to the hydroxybenzylidene must be protonated (53). However, the large effects on the chromophore of buried water molecules and the microenvironment supplied by the protein (52) would seem to provide a chemically more plausible explanation.

Two-Photon Excitation

One of the most promising new techniques in high-resolution fluorescence microscopy is two-photon excitation (54), in which two infrared photons hit a fluorophore within a few femtoseconds of each other and sum their energy to simulate a single photon of half the wavelength, that is, ultraviolet to blue. Such coincidence of infrared photons requires extremely high fluxes and therefore occurs to a significant extent only at the focus of a microscope objective of high numerical aperture, illuminated by a pulsed laser. Because other regions of the specimen are effectively not excited, they neither emit fluorescence nor are subject to photobleaching or photodynamic damage. As in confocal microscopy, the image is built up by scanning the focus point in a raster, but unlike confocal microscopy, out-of-focus planes are protected from bleaching, which is a tremendous advantage for two-photon excitation.

GFPs are quite good fluorophores for two-photon excitation. Wild-type GFP is readily excited with 780- to 800-nm pulses (43, 54–56), which are in the optimal output range for commercial mode-locked titanium-sapphire lasers. However, the photoisomerization proceeds just as with 390- to 400-nm single-photon excitation (55). Class 3 (neutral phenol) GFP mutants have not been tried but should be better because they disfavor photoisomerization. S65T, the prototypic class 2 GFP mutant, is optimally excited near 910 nm and has a slightly higher two-photon cross-section than the wild type (54). Two-photon excitation is also effective on class 6 (imidazole) blue mutants (43) as well as class 5 (indole) cyan mutants (H Fujisaki, G Fan, A Miyawaki, RY Tsien, unpublished observations).

Effects of pH

As noted above, wild-type GFP at high pH (11–12) loses absorbance and excitation amplitude at 395 nm and gains amplitude at 470 nm (8, 57). Such pH values, though mechanistically revealing, are almost never encountered in biology. Wild-type GFP is also quenched by acidic pH values with an apparent pK_a near 4.5. Several of the mutants with enhanced spectral properties at pH 7 are actually more acid sensitive than is the wild type; thus EGFP is 50% quenched at pH 5.5 (43). pK_as as high as 6.8 are found in some of the class 4 mutants with Thr203 replaced by an aromatic residue (J Llopis, RY Tsien, manuscript in preparation; R Wachter, SJ Remington, personal communication). The mechanistic explanation for these relatively high pK_as is not entirely clear. Loss of the Thr203 hydroxyl would indeed be expected to destabilize the phenolate form of the chromophore. However, the effect of acid is to quench the fluorescence altogether rather than simply shift it toward the short wavelengths expected of a protonated chromophore. The sensitivity of some GFPs to mildly acidic pH values carries both advantages and disadvantages. Such GFPs could be quenched to a major extent in acidic organelles such as lysosomes, endosomes, and Golgi compartments. The pH sensitivity of some GFPs can also be put to good use to measure organellar pH (J Llopis, RY Tsien, manuscript in preparation; R Wachter, SJ Remington, personal communication) by targeting appropriate GFPs to those locations.

Effects of Temperature and Protein Concentrations

Higher GFP concentrations amplify the main excitation peak at 395 nm at the expense of the subsidiary peak at 470 nm (8). Because the 395- and 470-nm peaks are believed to result from neutral and anionic fluorophores, respectively, aggregation probably inhibits ionization of the fluorophores. Increasing temperature from 15 to 65°C modestly decreases the 395-nm and increases the 470-nm excitation peak of mature wild-type GFP. Yet higher temperatures cause denaturation, with 50% of fluorescence lost at 78°C (8). As already mentioned, much more modest temperature increases from 20 to 37°C can profoundly decrease maturation efficiency of GFPs lacking mutations to improve folding.

Effects of Prior Illumination

GFPs have a variety of remarkable abilities to undergo photochemical transformations, which enables visualization of the diffusion or trafficking of GFP-tagged proteins. A defined zone within a cell or tissue is momentarily exposed to very bright illumination, which initiates the photochemistry. The subsequent fate of the photoconverted protein is imaged over time. At least four distinct types of semipermanent photochemical transformation have been reported from one or more GFPs: (*a*) simple irreversible photobleaching, (*b*) conversion from

a 395- to 475-nm excitation maximum, (*c*) loss of 488-nm-excited fluorescence, reversible by illumination at 406 nm, and (*d*) generation of rhodamine-like orange or red fluorescence upon illumination at 488 nm under strictly anaerobic conditions (58).

IRREVERSIBLE PHOTOBLEACHING Photobleaching is the simplest and most universal behavior of fluorophores. Most GFPs are relatively resistant to photobleaching (22, 59), perhaps because the fluorophore is well shielded from chemical reactants such as O_2. The bleach rate of the prototypic class 2 GFP, the S65T mutant, was reported to be relatively indifferent to equilibration with 0–100% oxygen or addition of quenchers of triplet states, singlet oxygen, and radicals (59). Nevertheless, with sufficient laser power, photobleaching is easily observed and exploited for measurements of fluorescence recovery (37, 59, 60). The class 6 mutants (BFPs) are generally more photosensitive than classes 1–5 (28). Cell-permeant antioxidants may be helpful in protecting such GFPs from bleaching. An example is Trolox, 6-hydroxy-2,5,7,8-tetramethylchroman-2-carboxylic acid, a water-soluble vitamin E analog commercially available from Aldrich Chemical Co., Milwaukee, WI.

SHIFTING TO A LONGER-WAVELENGTH EXCITATION PEAK This behavior is characteristic of wild-type and other class 1 GFPs (11, 22, 36). As discussed previously, the mechanism is probably a light-driven proton transfer from the neutral chromophore to the carboxylate of Glu222, yielding an anionic chromophore and a protonated Glu222 (32). This UV-induced enhancement of the blue excitation peak has been exploited to measure lateral diffusion of GFP-tagged proteins (37). Because the proton transfer is mediated by Thr203 and Ser205, mutation of those residues might be a promising way to enhance this photochromic effect. Indeed, UV irradiation of the double mutant T203S, S205T increases the amplitude of its long-wavelength excitation peak 11.8-fold, whereas wild-type GFP under the same conditions increases by at most 3.6-fold (R Heim, RY Tsien, unpublished information).

REVERSIBLE LOSS OF LONGER-WAVELENGTH EXCITATION PEAK; SINGLE MOLECULE DETECTION The opposite behavior, a shift from a longer to a shorter excitation wavelength, seems to occur in class 4 mutants. Upon intense laser illumination and observation of the fluorescence from single molecules immobilized in a polyacrylamide gel, such mutants both blink reversibly on a time scale of seconds and switch the fluorescence off over tens of seconds (61). However, the apparent bleaching can be reversed by illumination at short wavelengths such as 406 nm. Probably the chromophore, which is normally mostly anionic, can eventually be driven into a protonated state with an excitation maximum near 405 nm, whereupon it appears nonfluorescent and bleached to the probe

laser at 488 nm. However, excitation of the protonated state then restores the normal anionic state. Such cycling can be repeated many times with apparently no fatigue, so that it potentially represents a basis for an optical memory at the single molecule level. It might also be particularly advantageous for multiple determinations of diffusion or trafficking on the same region of interest.

ANAEROBIC PHOTOCONVERSION TO A RED FLUORESCENT SPECIES A variety of GFPs, including wild-type, S65T, and EGFP, undergo a remarkable photoconversion to a red fluorescent species under rigorously anaerobic conditions, for example, in microorganisms that have exhausted the oxygen in the medium, or in the presence of oxygen scavengers such as glucose plus glucose oxidase and catalase (58). The nature of this species emitting at 600 nm remains to be clarified. This effect has been used to measure the diffusibility of GFP in live bacteria. One complication is that the red emission develops with an exponential time constant of about 0.7 s after the illuminating flash (58).

EXPRESSION, FORMATION, MATURATION, RENATURATION, AND OBSERVATION

Promoters, Codon Usage, and Splicing

The expression level and detectability of GFP depend on many factors, the most important of which are summarized in Table 2. Obviously the more copies of the gene and the stronger the promoters/enhancers driving its transcription, the more protein that will be made per cell. In plants, it has been important to alter the original codon usage to eliminate a cryptic splice site (62). Codons have also been altered to conform to those preferred in mammalian systems (63, 64) and in the pathogenic yeast *Candida albicans* (65). Some authors have found such codon alterations to improve expression levels in mammalian systems (44, 63, 64), whereas others have found little improvement (43). Because the mammalianized genes are now widely available and may well be beneficial, they might as well be incorporated into all new GFP constructs for use in vertebrates. Our impression is that mammalian codons do not hurt expression levels in bacteria. Yet another improvement for mammalian systems is the inclusion of an optimal ribosome-binding site, also known as a Kozak sequence for translational initiation (66). Such a sequence requires insertion of an additional codon immediately after the starting methionine, as shown in Figure 1. The additional valine or alanine (40) does not seem to interfere with protein function; we prefer to number it 1a so that the numbering of the subsequent amino acids continues to correspond with the wild-type numbering. GFP can be expressed with reasonable efficiency in a cell-free in vitro translation system (67), a finding that confirms the protein can fold autonomously.

Table 2 Factors affecting the detectability of green fluorescent protein (GFP)

Total amount of GFP (picked out by antibodies, or by position on gel if GFP is abundant enough)
Number of copies of gene, duration of expression
Strength of transcriptional promotors and enhancers
Efficiency of translation including Kozak sequence and codon usage
Absence of mRNA splicing, protein degradation and export
Efficiency of posttranslational fluorophore formation
Solubility vs. formation of inclusion bodies
Availability of chaperones
Hindrance to folding because of unfortunate fusions to host proteins
Time, temperature, availability of O_2, and intrinsic rate of cyclization/oxidation
Molecular properties of mature GFP
Wavelengths of excitation and emission
Extinction coefficient and fluorescence quantum yield
Susceptibility to photoisomerization/bleaching
Dimerization
Competition with noise and background signals
Autofluorescence of cells or culture media at preferred wavelengths
Location of GFP, diffuse vs. confined to small subregions of cells or tissues
Quality of excitation and emission filters and dichroic mirrors
Sensitivity, noise, and dark current of photodetector

Folding Mutations and Thermotolerance

As mentioned previously, several mutations improve the ability of GFP to fold at temperatures above those to which the jellyfish would have been exposed. Most of them replace bulky residues with smaller ones. Their scattered locations throughout the three-dimensional structure of the mature protein (Figure 6) give little hint as to why they should help folding and maturation. Of course, the X-ray structures are all determined on well-folded mature proteins. At the stage when the mutations are needed, the protein is presumably less well ordered. As an alternative to mutating the GFP, the presence of chaperones can also help GFP fold (68). Aside from the potential technical importance of providing chaperones, this finding makes GFP a useful substrate for testing chaperone function (69), since GFP provides a continuous nondestructive assay for successful folding.

Requirement for O_2

The requirement for O_2 to dehydrogenate the α,β bond of residue 66 (21, 23, 24) means that GFP probably cannot become fluorescent in obligate anaerobes. So far this is the only fundamental limitation on the range of systems in which GFP can be expressed. Once GFP is matured, O_2 has no further effect (59). The oxidation seems to be the slowest step (Figure 2) in the maturation of GFP (23),

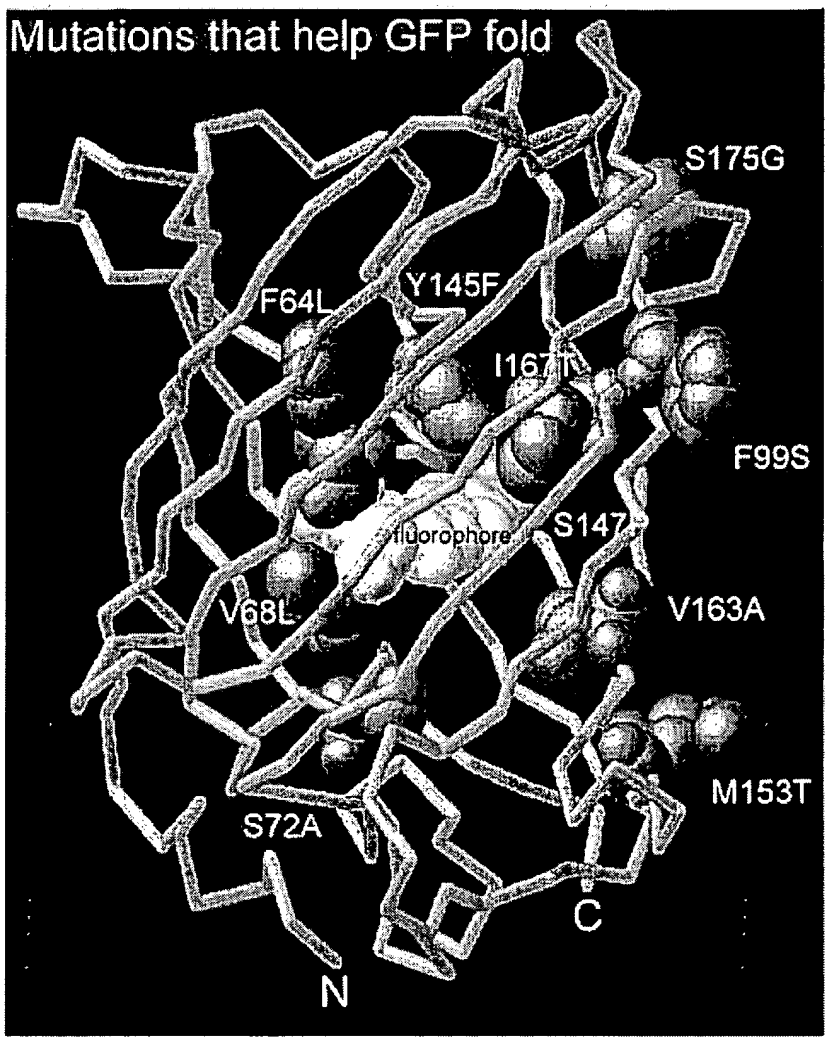

Figure 6 Location on the GFP crystal structure (30) of the most important sites that improve folding at 37°C. The amino acids shown in space-filling representation are the wild-type residues that are replaced by the mutations listed.

so it imposes the ultimate limit on the ability of GFP fluorescence to monitor rapid changes in gene expression. Considering its importance, surprisingly little work has been done on how to accelerate this oxidation. The dependence of rate on oxygen pressure has not been characterized, so it is unknown whether pO_2 higher than ordinary atmospheric would speed up the reaction. The mutant S65T has been reported to oxidize with an exponential time constant of 0.5 h, 4 times faster than the 2 h for wild-type protein under parallel conditions (25). Strong reductants such as dithionite can decolorize mature GFP (24, 52), probably by rehydrogenating the chromophore. Such reduction may also require that the GFP become denatured to allow access to the buried chromophore (23).

Histology in Fixed Tissues

Although the prime advantage of GFP is its ability to generate fluorescence in live tissue, its fluorescence does survive glutaraldehyde and formaldehyde fixatives (11). Occasional problems in maintaining fluorescence during fixation may result from uncontrolled acidity of the fixative solution or the use of excessive organic solvents, which denature the protein and destroy the fluorescence (7).

PASSIVE APPLICATIONS OF GFP

Cell biological applications of GFP may be divided into uses as a tag or as an indicator. In tagging applications, the great majority to date, GFP fluorescence merely reflects levels of gene expression or subcellular localizations caused by targeting domains or host proteins to which GFP is fused. As an indicator, GFP fluorescence can also be modulated posttranslationally by its chemical environment and protein-protein interactions.

Reporter Gene, Cell Marker

The first proposed application of GFP was to detect gene expression in vivo (11), especially in the nematode *Caenorhabditis elegans*, whose cuticle hinders access of the substrates required for detecting other reporter genes. GFP was particularly successful at confirming the pattern of expression of the *mec-7* promoter, which drives the formation of β-tubulin in a limited number of mechanosensory neurons. GFP's independence from enzymatic substrates is likewise particularly promising in intact transgenic embryos and animals (70–76) and for monitoring the effectiveness of gene transfer (48, 77, 78). However, GFP seems to need rather strong promoters to drive sufficient expression for detection, especially in mammalian cells. Most published examples, even those using brightened GFPs with mutations to promote folding at 37°C, have used constitutive promoters from viruses such as cytomegalovirus (CMV), SV40,

or HIV long terminal repeat (79), or strong exogenous regulators such as the tetracycline transactivator system (80, 81), rather than native genetic response elements modulated by endogenous signals.

The somewhat disappointing sensitivity of GFP as a so-called gene-tag is probably an inherent result of its lack of amplification. GFP is not an enzyme that catalytically processes an indefinite number of substrate molecules. Instead, each GFP molecule produces at most one fluorophore. It has been estimated that 1 μM well-folded wild-type GFP molecules are required to equal the endogenous autofluorescence of a typical mammalian cell (55), that is, to double the fluorescence over background. Mutant GFPs with improved extinction coefficients might improve this detection limit six- to tenfold (43) (see also Table 1), but 0.1 μM GFP is still approximately 10^5 copies per typical cell of 1–2 pL volume. This estimate already assumes perfect GFP maturation; imperfect or incomplete maturation would raise the threshold copy number even further. The ultimate sensitivity limit is set not by instrumentation but by cellular autofluorescence.

If cytosolic GFP is inadequately sensitive as a reporter gene, two alternatives should be considered. If the gene product can be detected by microscopic imaging with subcellular resolution, then targeting the GFP to a defined subcompartment of the cell can greatly reduce the number of molecules required. The GFP becomes highly concentrated, and the surrounding unlabeled region of the cell provides an internal reference for the autofluorescence background, which is usually diffuse in each cell. It is far easier to see local contrast within a cell than to quantitate a cell's average fluorescence relative to unlabeled standards. Thus as few as 300–3000 GFPs packed into a centrosome are readily visible as a green dot inside a cell (82). However, compartmentation of the GFP does not help with nonimaging detection methods such as fluorometry in cuvets or microtiter plates or fluorescence-activated cell sorting (FACS). A different solution is to use reporter gene products that can enzymatically catalyze a large change in the fluorescence of substrates that can be loaded into intact, fully viable cells. For example, the bacterial enzyme β-lactamase can be detected at levels as low as 60 pM in single mammalian cells (50 molecules per cell) with substrates loaded as membrane-permeant esters (83).

Fusion Tag

The most successful and numerous class of GFP applications has been as a genetic fusion partner to host proteins to monitor their localization and fate. The gene encoding a GFP is fused in frame with the gene encoding the endogenous protein and the resulting chimera expressed in the cell or organism of interest. The ideal result is a fusion protein that maintains the normal functions and localizations of the host protein but is now fluorescent. The range of successful

fusions is now much greater than previously tabulated (22). Not all fusions are successful, but the failures are almost never published, so it is difficult to assess the overall success rate. GFP has been targeted successfully to practically every major organelle of the cell, including plasma membrane (37, 84–87), nucleus (28, 38, 87–92), endoplasmic reticulum (50, 60, 93), Golgi apparatus (93), secretory vesicles (39, 94), mitochondria (28, 89, 95, 96), peroxisomes (97), vacuoles (98), and phagosomes (99). Thus the size and shape of GFP and the differing pHs and redox potentials of such organelles do not seem to impose any serious barrier. Even specific chromosomal loci can be tagged indirectly by inserting multiple copies of Lac operator sites and decorating them with a fusion of GFP with the Lac repressor protein (100). In general, fusions can be attempted at either the amino or carboxyl terminus of the host protein, sometimes with intervening spacer peptides. However, the crystal structures of GFP (30, 31) show that the N- and C-terminii of its core domain are not far apart, so it might be possible to splice GFP into a noncritical exterior loop or domain boundary of the host protein. For example, residues 2–233 of GFP have been inserted between the last transmembrane segment and the long cytoplasmic tail of a Shaker potassium channel (100a).

GFP AS AN ACTIVE INDICATOR

The rigid shell in GFP surrounding the chromophore enables it to be fluorescent and protects it from photobleaching but also hinders environmental sensitivity. Nevertheless, GFPs that act as indicators of their environment have been created by combinations of random and directed mutagenesis. The pH sensitivity of certain mutants and their potential application to measure organellar pH have already been mentioned. It is possible to engineer phosphorylation sites into GFP such that phosphorylation produces major changes in fluorescence under defined conditions (AB Cubitt, personal communication). The engineered fusion of GFP within the Shaker potassium channel is the first genetically encoded optical sensor of membrane potential (100a). Depolarization causes at most a 5% decrease in fluorescence with a time constant of approximately 85 ms, but both the amplitude and speed may well improve in future versions. But the most general way to make biochemically sensitive GFPs is to exploit fluorescence resonance energy transfer (FRET) between GFPs of different color. FRET is a quantum-mechanical phenomenon that occurs when two fluorophores are in molecular proximity (<100 Å apart) and the emission spectrum of one fluorophore, the donor, overlaps the excitation spectrum of the second fluorophore, the acceptor. Under these conditions, excitation of the donor can produce emission from the acceptor at the expense of the emission from the donor that would normally occur in the absence of the acceptor. Any biochemical signal that changes the distance between the fluorophores or relative orientation of their

transition dipoles will modulate the efficiency of FRET (101–103). Because FRET is a through-space effect, it is not necessary to perturb either GFP alone but rather only the linkage or spatial relationship between them. The potential utility of FRET between GFPs was the main motivation for the development of most of the mutations in Table 1. The change in ratio of acceptor to donor emissions is nearly ideal for cellular imaging and flow cytometry because the two emissions can be obtained simultaneously and their ratio cancels out variations in the absolute concentration of the GFPs, the thickness of the cell, the brightness of the excitation source, and the absolute efficiency of detection. Because the sample need be excited at only one wavelength, which should preferentially excite the donor, FRET is ideal for laser-scanning confocal microscopy and FACS (103). FRET also causes changes in donor fluorescence lifetime and bleaching rate (104), but detection of those signals either requires much more sophisticated instrumentation or is destructive.

Protease Action

The simplest and first-demonstrated way to achieve and modulate FRET between GFPs was to fuse a blue-emitting (class 6) GFP mutant (i.e. a BFP) to a phenolate-containing (class 2) green GFP via an intervening protease-sensitive spacer (41, 105). The broad emission spectrum of the donor BFP, peaking at 447 nm, overlaps fairly well with the excitation spectrum of the class 2 GFP, peaking at 489 nm. Wild-type GFP would not be satisfactory, because the 383 nm used to excite the BFP would directly and efficiently excite the 395-nm excitation peak of wild-type GFP even in the absence of FRET. The tandem fusion exhibits FRET, which is then disrupted when a protease is added to cleave the spacer and let the GFPs diffuse apart. Heim & Tsien (41) used P4-3 and S65C or S65T and a trypsin- or enterokinase-sensitive 25-residue linker, and achieved a 4.6-fold increase in the ratio of blue to green emissions resulting from protease action. Control experiments verified that the two GFPs were unaffected by the proteases at the concentrations used, so the spectral change reflected cleavage of the linker. Mitra et al (105) used BFP5 (F64M, Y66H) and RSGFP4 with a Factor X_a-sensitive linker and obtained a 1.9-fold increase in the analogous ratio. Although FRET-based assays for proteases are well known (106, 107), synthetic peptide substrates are limited in length and useful only in vitro. The special advantages of GFP-based constructs are that they could incorporate full-length protein substrates and could be expressed and assayed inside live cells or organisms.

Transcription Factor Dimerization

A static homodimerization of the transcription factor Pit-1 has been detected by coexpression of BFP-Pit-1 and GFP-Pit-1 fusions in HeLa cells. Homodimerization is inherently more difficult than heterodimerization to demonstrate

by FRET, because at most 50% of the complexes will combine BFP- and GFP-labeled proteins, while nonproductive BFP-BFP and GFP-GFP complexes will each account for 25% of the homodimers. Nevertheless, careful spectral analysis indicated that homodimerization was detectable by FRET (108). Unfortunately, no modulation of the Pit-1 interaction or new biological conclusions were reported.

Ca^{2+} Sensitivity

The first dynamically responsive biochemical indicators based on GFP are Ca^{2+} sensors, independently developed almost simultaneously by Romoser et al (109) and by Miyawaki et al (50). Romoser et al linked commercially available class 6 BFP and class 2 GFP mutants with a 26-residue spacer containing the calmodulin (CaM)-binding domain from avian smooth muscle myosin light chain kinase. This spacer allowed FRET to occur from the BFP to the GFP, perhaps because it was long and flexible enough for the two GFPs to dimerize. Addition of Ca^{2+}-CaM disrupted FRET, presumably by binding to and straightening the linker so that the two GFPs were unable to dimerize. Such binding of Ca^{2+}-CaM decreased the 505 nm emission by 65% and the ratio of 505- to 440-nm emissions by sixfold in vitro, an impressive spectral change for a reversible conformational change less drastic than proteolytic cleavage. The bacterially expressed recombinant protein was then microinjected into individual HEK-293 cells. In such intact cells, elevations of cytosolic free Ca^{2+} produced much more modest decreases (5–10%) in 510-nm emission, which could be amplified to about 30% decreases if exogenous calmodulin was co-injected. Thus the response of the indicator in cells was limited by CaM availability, implying that the indicator is responsive to cellular Ca^{2+}-CaM rather than Ca^{2+} per se. Because the heterologously expressed protein had to be microinjected, the unique ability of GFP to be continuously synthesized by the target cell was not exploited, and only cytosolic signals could be monitored.

Miyawaki et al (50) fused BFP or class 5 cyan-fluorescent protein (CFP) to the N-terminus of CaM, and class 2 GFP or class 4 yellow-fluorescent protein (YFP) to the C-terminus of M13, the CaM-binding peptide from skeletal muscle myosin light chain kinase. The CFP-CaM and the M13-YFP could either be fused via two glycines (in which case all four protein domains were joined into a 76-kDa tandem chimera) or left separate. In either case, binding of Ca^{2+} to the CaM caused it to grab the M13, thus increasing FRET, the opposite spectral effect from that of Romoser et al (109). By using GFPs with mutations to optimize mammalian expression, the indicators were bright enough to be introduced into cells by DNA transfection rather than protein microinjection. Because the four-domain chimeras were expressed in situ, they could readily be targeted to organelles such as the nucleus or endoplasmic reticulum by addition

Table 3 Advantages and disadvantages of GFP-based Ca^{2+} indicators[a]

Advantages
Applicable to nearly all organisms; no need for ester permeation and hydrolysis
Can be targeted to specific tissues, cells, organelles, or proteins
Unlikely to diffuse well enough to blur spatial gradients
Modular construction is readily modified/improved by mutagenesis
Good optical properties: visible excitation, emission ratioing, high photostability
cDNAs or improved sequences are cheap to replicate and distribute
Should be generalizable to measure many bioactive species other than Ca^{2+}, as long as a conformationally sensitive receptor is available
Disadvantages
Gene transfection required
The maximum change in emission ratio is currently less than for small-molecule dyes
The binding kinetics are somewhat slower
The CaM or M13 might have some additional biological activity

[a]GFP, green fluorescent proteins.

of appropriate targeting sequences. Ca^{2+} affinities were readily adjustable by mutation of the CaM. Thus free Ca^{2+} concentrations in the endoplasmic reticulum were measured to be 60–400 μM in unstimulated cells, decreasing to 1–50 μM in cells treated with Ca^{2+}-mobilizing agonists. Advantages and disadvantages of the GFP-based Ca^{2+} indicators (called cameleons) compared to conventional Ca^{2+} indicators are summarized in Table 3.

The constructs with separate CFP-CaM and M13-YFP proved that FRET between GFP mutants can dynamically monitor protein-protein interaction in single living cells. Binding of the two host proteins to each other brings their fused GFPs into proximity and enhances FRET. By comparison the mechanism of Romoser et al (109) requires that mutual binding must substantially change the distance between N- and C-terminii of at least one of the partners.

In principle the use of FRET offers some major advantages and disadvantages over other current methods for detecting protein-protein interaction (Table 4). The most unique advantages are the spatial and temporal resolution and the ability to observe the proteins in any compartment of the cell. The biggest disadvantage is that even in the absence of any protein interaction, a substantial background signal is present when illuminating at the donor's excitation maximum and observing at the acceptor's emission maximum. This background signal arises because the donor emission has a tail that extends into the acceptor's emission band, and the acceptor excitation has a tail that extends into the donor's excitation band. For these reasons, FRET is probably not a suitable method for detecting trace interactions or fishing for unknown partners but

Table 4 Advantages and disadvantages of FRET between (GFPs) to monitor protein interactions.

Advantages
Works in vitro and in living mammalian cells, not just yeast
Can respond dynamically to posttranslational modifications
Has high temporal (milliseconds) and spatial (submicron) resolution
Interacting proteins can be anywhere in the cell and do not need to be sent to nucleus
Degree of association can be quantified, if 0% and 100% binding can be established in situ
Efficiency of FRET at 100% complexation gives some structural information
Disadvantages of intermolecular FRET
Must express fusion proteins, in which host protein and GFPs must both remain functional
If GFPs are too far from each other ($\gg$80 Å) or unluckily oriented, FRET will fail
Even with no association, spectral overlap contributes some signal at the FRET wavelengths
Trace or rare interactions will be hard to detect
Need negative and positive controls, i.e. reference conditions of 0% and 100% association
Homodimerization is more difficult to monitor than heterodimerization

is best used at a later stage when the two host proteins are molecularly well characterized and the detailed spatiotemporal dynamics of their interaction is to be determined in live cells.

What Are the Best FRET Partners?

The efficiency of FRET is given by the expression $R_0^6/(R_0^6 + r^6)$, where r is the actual distance between the centers of the chromophores and R_0 is the distance at which FRET is 50% efficient. R_0 depends on the quantum yield of the donor, the extinction coefficient of the acceptor, the overlap of the donor emission and acceptor excitation spectra, and the mutual orientation of the chromophores (102). The early attempts to obtain FRET between GFPs all used BFPs (class 6 mutants) as donors and class 2 (phenolate anion) GFPs as acceptors because these were the first available pairs with sufficiently distinct wavelengths. For such pairs, R_0 is calculated to range from 40 to 43 Å. However, the poor extinction coefficients, quantum yields, and photostabilities of the BFPs have convinced us (50) that cyan mutants (class 5) are much better donors. The acceptor correspondingly must become a class 4 yellow mutant so that its excitation spectrum overlaps the donor emission as much as possible, whereas the two emissions remain as distinct as possible. Combinations of cyan donors with yellow acceptors have R_0 values of 49–52 Å and are our currently preferred donor-acceptor pairs. So far, the highest value of R_0 between two GFPs is 60 Å for class 3 mutant H9-40 as donor to Topaz, but unfortunately these mutants' emission spectra are too close to each other for good discrimination.

The above calculations have assumed that the GFPs are randomly oriented or tumbling with respect to one another, which is the conventional assumption

Table 4 Advantages and disadvantages of FRET between (GFPs) to monitor protein interactions.

Advantages
Works in vitro and in living mammalian cells, not just yeast
Can respond dynamically to posttranslational modifications
Has high temporal (milliseconds) and spatial (submicron) resolution
Interacting proteins can be anywhere in the cell and do not need to be sent to nucleus
Degree of association can be quantified, if 0% and 100% binding can be established in situ
Efficiency of FRET at 100% complexation gives some structural information
Disadvantages of intermolecular FRET
Must express fusion proteins, in which host protein and GFPs must both remain functional
If GFPs are too far from each other ($\gg$80 Å) or unluckily oriented, FRET will fail
Even with no association, spectral overlap contributes some signal at the FRET wavelengths
Trace or rare interactions will be hard to detect
Need negative and positive controls, i.e. reference conditions of 0% and 100% association
Homodimerization is more difficult to monitor than heterodimerization

is best used at a later stage when the two host proteins are molecularly well characterized and the detailed spatiotemporal dynamics of their interaction is to be determined in live cells.

What Are the Best FRET Partners?

The efficiency of FRET is given by the expression $R_0^6/(R_0^6 + r^6)$, where r is the actual distance between the centers of the chromophores and R_0 is the distance at which FRET is 50% efficient. R_0 depends on the quantum yield of the donor, the extinction coefficient of the acceptor, the overlap of the donor emission and acceptor excitation spectra, and the mutual orientation of the chromophores (102). The early attempts to obtain FRET between GFPs all used BFPs (class 6 mutants) as donors and class 2 (phenolate anion) GFPs as acceptors because these were the first available pairs with sufficiently distinct wavelengths. For such pairs, R_0 is calculated to range from 40 to 43 Å. However, the poor extinction coefficients, quantum yields, and photostabilities of the BFPs have convinced us (50) that cyan mutants (class 5) are much better donors. The acceptor correspondingly must become a class 4 yellow mutant so that its excitation spectrum overlaps the donor emission as much as possible, whereas the two emissions remain as distinct as possible. Combinations of cyan donors with yellow acceptors have R_0 values of 49–52 Å and are our currently preferred donor-acceptor pairs. So far, the highest value of R_0 between two GFPs is 60 Å for class 3 mutant H9-40 as donor to Topaz, but unfortunately these mutants' emission spectra are too close to each other for good discrimination.

The above calculations have assumed that the GFPs are randomly oriented or tumbling with respect to one another, which is the conventional assumption

made in calculating R_0 (102). If instead the mutual orientation of the two chromophores were the same as in the crystal structure for the wild-type dimer (31), the R_0s would be about 72% of the previously calculated values, for example, 35–37 Å for cyan-to-yellow FRET. For comparison, the actual distance r between the centers of the chromophores in the dimer is about 25 Å, which would predict that FRET would occur with about 90% efficiency in such a direct heterodimer between cyan and yellow mutants.

OUTLOOK FOR FUTURE RESEARCH

Despite all that has been learned about how GFP works and how it can be exploited as a research tool, enormous challenges and opportunities remain. Listed below are some unanswered general questions about GFP that are among the most intriguing, excluding problems related to narrow applications in cell biology:

Cloning of Related GFPs

What are the genetic sequences and structures of GFP homologs from bioluminescent organisms other than *Aequorea*? This information would illuminate the evolution of fluorescent proteins, reveal the essential conserved elements of the structure, and provide the genetic raw material for combinatorial mixing and matching to produce hybrid proteins with new phenotypes. *Renilla* GFP is the most obvious next cloning target, but even more bioluminescent organisms should be investigated.

Protein Folding and Chromophore Folding

We need to know much more about how GFP folds into its β-barrel conformation and synthesizes its internal chromophore. Now that many of the steps have been kinetically resolved (23), the effect of mutations on each of the steps needs to be determined. The most informative mutants will not be the majority that completely prevent the formation of fluorescence, because those could act anywhere in the entire cascade including disruption of the final state. Instead, mutants or chaperonins that affect the rates but not the final extent of fluorescence development are likely to be most valuable. The molecular mechanism, kinetics, and byproducts of chromophore formation by O_2 are particularly critical questions.

Altered Wavelengths of Fluorescence

Yet longer wavelengths of excitation and emission than are currently available from the class 4 (π-stacked phenolate) mutants (Table 1) would be useful for multiple labels and reporters and to serve as resonance energy transfer acceptors.

For example, an increase in excitation maximum to 540–550 nm would permit efficient energy transfer from terbium chelates, whose millisecond excited-state lifetimes make them useful as energy transfer donors (110). The 560–570 nm emission from such longer-wavelength GFP mutants would also be distinct enough from the standard class 2 (phenolate) mutants to make such green-orange pairs useful as FRET partners. Another approach to improving FRET would be to reduce the emission bandwidth of the class 5 (tryptophan-based) cyan mutants and thereby improve the quantitative separation of cyan and yellow emissions. Emission spectral alterations should be most easily screened by fluorescence-activated cell sorting (FACS). The chemical structure of the red fluorescent species formed by intense illumination in anaerobic conditions (58) must be determined as the first step in making this extraordinary photochemical reaction more general and useful.

Altered Chemical and Photochemical Sensitivities

The sensitivity of GFP spectra to environmental factors such as pH and past illumination is valuable if pH indication or photochemical tagging is desired but is a nuisance for most other applications. Therefore we need to understand the molecular mechanisms of such environmental modulations and to find mutations that enhance or eliminate those mechanisms. In many cases, it will be important to use screening methods that, unlike FACS, permit longitudinal comparison of individual cells or colonies before and after a chemical or actinic challenge. Digital imaging of colonies on plates (e.g. 111) is likely to be advantageous.

Fusions Other Than at N- or C-Terminus

Almost all fusions of host proteins with GFP have been simple tandem fusions in which the C-terminus of one protein is genetically concatenated to the N-terminus of the other. Because not all such fusions work, general rules are needed in order to predict when fluorescence will be intact and when host protein function will be preserved. Sometimes neither order of simple concatenation produces functional chimeras. Could splicing of GFP into the middle of the host protein be made easier and more general? It might be helpful to engineer GFP to move its N- and C-terminii as close to each other as possible, perhaps by addition of spacers or by circular permutation.

Alternatives to Fluorescence

Chromophores can be harnessed to perform many functions other than fluorescence, such as phosphorescence (emission from the triplet state), generation of reactive oxygen species such as singlet oxygen or hydroxyl radical, and photochemical cleavage. Can GFP be engineered to do such tricks? Phosphorescence

typically gives lifetimes in microseconds rather than nanoseconds and therefore permits exploration of protein dynamics on longer time scales. Controlled generation of singlet oxygen can be useful to polymerize diaminobenzidine locally into a polymer visible by electron microscopy, so that the location of fluorophores can be verified at ultrastructural resolution (112). Laser pulses can be used to kill proteins within a few nanometers of a suitable chromophore that generates hydroxyl radicals or other reactive species (113). Photochemical cleavage is the basis of important methods to produce sudden changes in the concentration of signaling molecules (114). These techniques would be revolutionized if their crucial molecules could be synthesized or at least localized in situ under molecular biological control, in the same way as GFP. Of course, the rigid shell protecting the chromophore of GFP from the environment may intrinsically prevent even mutagenized GFPs from fulfilling such alternative functions, so that completely different proteins may need to be found or devised. Perhaps GFP will become just one prototype of a collection of genetically encoded, light-driven macromolecular reagents.

ACKNOWLEDGMENTS

I thank the many collaborators and colleagues who allowed me to cite their unpublished results or manuscripts in preparation. The Howard Hughes Medical Institute and the National Institutes of Health (NS27177) provided essential financial support.

Literature Cited

1. Shimomura O, Johnson FH, Saiga Y. 1962. *J. Cell. Comp. Physiol.* 59:223–39
2. Johnson FH, Shimomura O, Saiga Y, Gershman LC, Reynolds GT, Waters JR. 1962. *J. Cell. Comp. Physiol.* 60:85–103
3. Morin JG, Hastings JW. 1971. *J. Cell. Physiol.* 77:313–18
4. Morise H, Shimomura O, Johnson FH, Winant J. 1974. *Biochemistry* 13:2656–62
5. Prendergast FG, Mann KG. 1978. *Biochemistry* 17:3448–53
6. Shimomura O. 1979. *FEBS Lett.* 104: 220–22
7. Ward WW, Cody CW, Hart RC, Cormier MJ. 1980. *Photochem. Photobiol.* 31:611–15
8. Ward WW, Prentice HJ, Roth AF, Cody CW, Reeves SC. 1982. *Photochem. Photobiol.* 35:803–8
9. Ward WW, Bokman SH. 1982. *Biochemistry* 21:4535–40
10. Prasher DC, Eckenrode VK, Ward WW, Prendergast FG, Cormier MJ. 1992. *Gene* 111:229–33
11. Chalfie M, Tu Y, Euskirchen G, Ward WW, Prasher DC. 1994. *Science* 263:802–5
12. Inouye S, Tsuji FI. 1994. *FEBS Lett.* 341:277–80
13. Ward WW. 1979. In *Photochemical and Photobiological Reviews*, ed. KC Smith, 4:1–57. New York: Plenum
14. Ward WW, Cormier MJ. 1979. *J. Biol. Chem.* 254:781–88
15. Lee J, Gibson BG, O'Kane DJ, Kohnle A, Bacher A. 1992. *Eur. J. Biochem.*

210:711–19
16. Macheroux P, Schmidt KU, Steinerstauch P, Ghisla S. 1987. *Biochem. Biophys. Res. Commun.* 146:101–6
17. Glazer AN. 1989. *J. Biol. Chem.* 264:1–4
18. Song P-S, Koka P, Prézelin BB, Haxo FT. 1976. *Biochemistry* 15:4422–27
19. Tsien RY, Prasher DC. 1997. In *GFP: Green Fluorescent Protein Strategies and Applications*, ed. M Chalfie, S Kain. New York: Wiley & Sons
20. Cody CW, Prasher DC, Westler WM, Prendergast FG, Ward WW. 1993. *Biochemistry* 32:1212–18
21. Heim R, Prasher DC, Tsien RY. 1994. *Proc. Natl. Acad. Sci. USA* 91:12501–4
22. Cubitt AB, Heim R, Adams SR, Boyd AE, Gross LA, Tsien RY. 1995. *Trends Biochem. Sci.* 20:448–55
23. Reid BG, Flynn GC. 1997. *Biochemistry* 36:6786–91
24. Inouye S, Tsuji FI. 1994. *FEBS Lett.* 351:211–14
25. Heim R, Cubitt AB, Tsien RY. 1995. *Nature* 373:663–64
26. Kojima S, Hirano T, Niwa H, Ohashi M, Inouye S, Tsuji FL. 1997. *Tetrahedron Lett.* 38:2875–78
27. Wright HT. 1991. *Crit. Rev. Biochem. Mol. Biol.* 26:1–52
28. Rizzuto R, Brini M, DeGiorgi F, Rossi R, Heim R, et al. 1996. *Curr. Biol.* 6:183–88
29. Perozzo MA, Ward KB, Thompson RB, Ward WW. 1988. *J. Biol. Chem.* 263:7713–16
30. Ormö M, Cubitt AB, Kallio K, Gross LA, Tsien RY, Remington SJ. 1996. *Science* 273:1392–95
31. Yang F, Moss LG, Phillips GN Jr. 1996. *Nat. Biotechnol.* 14:1246–51
32. Brejc K, Sixma TK, Kitts PA, Kain SR, Tsien RY, et al. 1997. *Proc. Natl. Acad. Sci. USA* 94:2306–11
33. Palm GJ, Zdanov A, Gaitanaris GA, Stauber R, Pavlakis GN, Wlodawer A. 1997. *Nat. Struct. Biol.* 4:361–65
34. Wachter RM, King BA, Heim R, Kallio K, Tsien RY, et al. 1997. *Biochemistry* 36:9759–65
34a. Phillips GN Jr. 1997. *Curr. Opin. Struct. Biol.* 7:821–27
35. Dopf J, Horiagon TM. 1996. *Gene* 173: 39–44
36. Chattoraj M, King BA, Bublitz GU, Boxer SG. 1996. *Proc. Natl. Acad. Sci. USA* 93:8362–67
37. Yokoe H, Meyer T. 1996. *Nat. Biotechnol.* 14:1252–56
38. Lim CR, Kimata Y, Oka M, Nomaguchi K, Kohno K. 1995. *J. Biochem.* 118:13–17
39. Kaether C, Gerdes HH. 1995. *FEBS Lett.* 369:267–71
40. Crameri A, Whitehorn EA, Tate E, Stemmer WPC. 1996. *Nat. Biotechnol.* 14:315–19
41. Heim R, Tsien RY. 1996. *Curr. Biol.* 6:178–82
42. Kahana J, Silver P. 1996. In *Current Protocols in Molecular Biology*, ed. FM Ausabel, R Brent, RE Kingston, DD Moore, JG Seidman, et al, 9(7):22–28 New York: Wiley & Sons
43. Patterson GH, Knobel SM, Sharif WD, Kain SR, Piston DW. 1997. *Biophys. J.* 73:2782–90
44. Cubitt AB, Heim R, Woollenweber LA. 1997. *Methods Cell Biol.* In press
45. Ward WW. 1997. In *Green Fluorescent Protein: Properties, Applications, and Protocols*, ed. M Chalfie, S Kain. New York: John Wiley & Sons
46. Delagrave S, Hawtin RE, Silva CM, Yang MM, Youvan DC. 1995. *Bio-Technology* 13:151–14
47. Cormack BP, Valdivia RH, Falkow S. 1996. *Gene* 173:33–38
48. Cheng LZ, Fu J, Tsukamoto A, Hawley RG. 1996. *Nat. Biotechnol.* 14:606–9
49. Ehrig T, O'Kane DJ, Prendergast FG. 1995. *FEBS Lett.* 367:163–66
50. Miyawaki A, Llopis J, Heim R, McCaffery JM, Adams JA, et al. 1997. *Nature* 388:882–87
51. Wu C, Liu HZ, Crossen R, Gruenwald S, Singh S. 1997. *Gene* 190:157–62
52. Niwa H, Inouye S, Hirano T, Matsuno T, Kojima S, et al. 1996. *Proc. Natl. Acad. Sci. USA* 93:13617–22
53. Voityuk AA, Michel-Beyerle ME, Rösch N. 1997. *Chem. Phys. Lett.* 272: 162–67
54. Xu C, Zipfel W, Shear JB, Williams RM, Webb WW. 1996. *Proc. Natl. Acad. Sci. USA* 93:10763–68
55. Niswender KD, Blackman SM, Rohde L, Magnuson MA, Piston DW. 1995. *J. Microsc.* 180:109–16
56. Potter SM, Wang C-M, Garrity PA, Fraser SE. 1996. *Gene* 173:25–31
57. Bokman SH, Ward WW. 1981. *Biochem. Biophys. Res. Commun.* 101:1372–80
58. Elowitz MB, Surette MG, Wolf E, Stock J, Leibler S. 1997. *Curr. Biol.* 7:809–12
59. Swaminathan KS, Hoang CP, Verkman AS. 1997. *Biophys. J.* 72:1900–7
60. Subramanian K, Meyer T. 1997. *Cell* 89: 963–71

61. Dickson RM, Cubitt AB, Tsien RY, Moerner WE. 1997. *Nature* 388:355–58
62. Haseloff J, Siemering KR, Prasher DC, Hodge S. 1997. *Proc. Natl. Acad. Sci. USA* 94:2122–27
63. Zolotukhin S, Potter M, Hauswirth WW, Guy J, Muzyczka N. 1996. *J. Virol.* 70: 4646–54
64. Yang T-T, Cheng L, Kain SR. 1996. *Nucleic Acids Res.* 24:4592–93
65. Cormack BP, Bertram G, Egerton M, Gow NAR, Falkow S, Brown AJP. 1997. *Microbiology* 143:303–11
66. Kozak M. 1989. *J. Cell Biol.* 108:229–41
67. Kahn TW, Beachy RN, Falk MM. 1997. *Curr. Biol.* 7:R207–8
68. Weissman JS, Rye HS, Fenton WA, Beechem JM, Horwich AL. 1996. *Cell* 84:481–90
69. Makino Y, Amada K, Taguchi H, Yoshida M. 1997. *J. Biol. Chem.* 272:12468–74
70. Ikawa M, Kominami K, Yoshimura Y, Tanaka K, Nishimune Y, Okabe M. 1995. *Dev. Growth Differ.* 37:455–59
71. Zernicka-Goetz M, Pines J, Hunter SM, Dixon JPC, Siemering KR, et al. 1997. *Development* 124:1133–37
72. Chiocchetti A, Tolosano E, Hirsch E, Silengo L, Altruda F. 1997. *Biochim. Biophys. Acta* 1352:193–202
73. Gagneten S, Le Y, Miller J, Sauer B. 1997. *Nucleic Acids Res.* 25:3326–31
74. Takada T, Iida K, Awaji T, Itoh K, Takahashi R, et al. 1997. *Nat. Biotechnol.* 15:458–61
75. Ikawa M, Kominami K, Yoshimura Y, Tanaka K, Nishimune Y, Okabe M. 1995. *FEBS Lett.* 375:125–28
76. Amsterdam A, Lin S, Moss LG, Hopkins N. 1996. *Gene* 173:99–103
77. Muldoon RR, Levy JP, Kain SR, Kitts PA, Link CJJ. 1997. *BioTechniques* 22: 162–67
78. Zhang GH, Gurtu V, Kain SR. 1996. *Biochem. Biophys. Res. Commun.* 227: 707–11
79. Gervaix A, West D, Leoni LM, Richman DD, Wong-Staal F, Corbeil J. 1997. *Proc. Natl. Acad. Sci. USA* 94:4653–58
80. Anderson MT, Tjioe IM, Lorincz MC, Parks DR, Herzenberg LA, Nolan GP. 1996. *Proc. Natl. Acad. Sci. USA* 93: 8508–11
81. Mosser DD, Caron AW, Bourget L, Jolicoeur P, Massie B. 1997. *BioTechniques* 22:150–61
82. Shelby RD, Hahn KM, Sullivan KF. 1996. *J. Cell Biol.* 135:545–57
83. Zlokarnik G, Negulescu PA, Knapp TE, Santiso-Mere D, Burres N, et al. 1998 *Science* 279:84–88
84. Marshall J, Molloy R, Moss GWJ, Howe JR, Hughes TE. 1995. *Neuron* 14:211–15
85. Barak LS, Ferguson SSG, Zhang J, Martenson C, Meyer T, Caron MG. 1997. *Mol. Pharmacol.* 51:177–84
86. Moriyoshi K, Richards LJ, Akazawa C, O'Leary DDM, Nakanishi S. 1996. *Neuron* 16:255–60
87. Hanakam F, Albrecht R, Eckerskorn C, Matzner M, Gerisch G. 1996. *EMBO J.* 15:2935–43
88. Grebenok RJ, Pierson E, Lambert GM, Gong F-C, Afonso CL, et al. 1997. *Plant J.* 11:573–86
89. DeGiorgi F, Brini M, Bastianutto C, Marsault R, Montero M, et al. 1996. *Gene* 173:113–17
90. Corbett AH, Koepp DM, Schlenstedt G, Lee MS, Hopper AK, Silver P. 1995. *J. Cell Biol.* 130:1017–26
91. Carey KL, Richards SA, Lounsbury KM, Macara IG. 1996. *J. Cell Biol.* 133: 985–96
92. Chatterjee S, Stochaj U. 1996. *BioTechniques* 21:62–63
93. Presley JF, Cole NB, Schroer TA, Hirschberg K, Zaal KJM, Lippincott-Schwartz J. 1997. *Nature* 389:81–85
94. Lang T, Wacker I, Steyer J, Kaether C, Wunderlich I, et al. 1997. *Neuron* 18:857–63
95. Murray AW, Kirschner MW. 1989. *Science* 246:614–21
96. Yano M, Kanazawa M, Terada K, Namchai C, Yamaizumi M, et al. 1997. *J. Biol. Chem.* 272:8459–65
97. Wiemer EAC, Wenzel T, Deerinck TJ, Ellisman MH, Subramani S. 1997. *J. Cell Biol.* 136:71–80
98. Cowles CR, Odorizzi G, Payne GS, Emr SD. 1997. *Cell* 91:109–18
99. Maniak M, Rauchenberger R, Albrecht R, Murphy J, Gerisch G. 1995. *Cell* 83: 915–24
100. Straight AF, Marshall WF, Sedat JW, Murray AW. 1997. *Science* 277:574–78

100a. Siegel MS, Isacoff EY. 1997. *Neuron* 19:735–41

101. Stryer L. 1978. *Annu. Rev. Biochem.* 47: 819–46
102. Lakowicz JR. 1983. *Principles of Fluorescence Spectroscopy.* New York: Plenum

103. Tsien RY, Bacskai BJ, Adams SR. 1993. *Trends Cell Biol.* 3:242–45
104. Jovin TM, Arndt-Jovin DJ. 1989. *Annu. Rev. Biophys. Biophys. Chem.* 18:271–308
105. Mitra RD, Silva CM, Youvan DC. 1996. *Gene* 173:13–17
106. Krafft GA, Wang GT. 1994. *Methods Enzymol.* 241:70–86
107. Knight CG. 1995. *Methods Enzymol.* 248:18–34
108. Periasamy A, Kay SA, Day RN. 1997. In *Functional Imaging and Optical Manipulation of Living Cells, Proc. SPIE 2983*, ed. DL Farkas, BJ Tromberg. Bellingham, WA: SPIE
109. Romoser VA, Hinkle PM, Persechini A. 1997. *J. Biol. Chem.* 272:13270–74
110. Selvin PR. 1996. *IEEE J. Sel. Top. Quant. Electron.* 2:1077–87
111. Youvan DC, Goldman ER, Delgrave S, Yang MM. 1995. *Methods Enzymol.* 246:732–48
112. Deerinck TJ, Martone ME, Lev-Ram V, Green DPL, Tsien RY, et al. 1994. *J. Cell Biol.* 126:901–10
113. Linden KG, Liao JC, Jay DG. 1992. *Biophys. J.* 61:956–62
114. Adams SR, Tsien RY. 1993. *Annu. Rev. Physiol.* 55:755–84

CREATING NEW FLUORESCENT PROBES FOR CELL BIOLOGY

Jin Zhang[*], *Robert E. Campbell*[*], *Alice Y. Ting*[*‡] *and Roger Y. Tsien*[*§]

Fluorescent probes are one of the cornerstones of real-time imaging of live cells and a powerful tool for cell biologists. They provide high sensitivity and great versatility while minimally perturbing the cell under investigation. Genetically-encoded reporter constructs that are derived from fluorescent proteins are leading a revolution in the real-time visualization and tracking of various cellular events. Recent advances include the continued development of 'passive' markers for the measurement of biomolecule expression and localization in live cells, and 'active' indicators for monitoring more complex cellular processes such as small-molecule-messenger dynamics, enzyme activation and protein–protein interactions.

PHOTOBLEACHING
The irreversible destruction, by any one of a number of different mechanisms, of a fluorophore that is under illumination.

[*]*Department of Pharmacology and* [§]*Department of Chemistry & Biochemistry and Howard Hughes Medical Institute, University of California, San Diego, 9500 Gilman Drive, La Jolla, California 92093–0647, USA.*
[‡]*Department of Chemistry, Massachusetts Institute of Technology, 77 Massachusetts Avenue, 18–496, Cambridge, Massachusetts 02139, USA.*
Correspondence to R.Y.T
e-mail: rtsien@ucsd.edu
doi:10.1038/nrm976

Our understanding of biological systems is increasingly dependent on our ability to visualize and quantify signalling molecules and events with high spatial and temporal resolution in the cellular context. Advances in fluorescence microscopy and the engineering of the green fluorescent protein (GFP) from *Aequorea victoria* into mutants with improved properties and altered colours have provided the basic tools that allow the investigation of more complex processes in live cells. The primary advantages of fluorescent protein-based indicators over simple organic dyes are that they can be designed to respond to a much greater variety of biological events and signals, targeted to subcellular compartments, introduced into a wider variety of tissues and intact organisms, and they very rarely cause photodynamic toxicity. This review highlights recent advances in the development of fluorescent probes for cellular applications, and focuses on those that can resolve spatial and temporal patterns through targeting to subcellular compartments. As the number of successful genetically-encoded reporters increases, several design trends and considerations are becoming apparent (BOX 1). We highlight the most versatile and modular of these designs as the blueprints for the construction of new and better reporters.

Recent advances in fluorescent proteins

New variants of green fluorescent protein. There is a continuing effort to develop new GFP variants with altered excitation and emission wavelengths, enhanced brightness and an improved pH resistance relative to the original enhanced green (for example, S65T and EGFP), cyan (CFP), and yellow (YFP) variants[1–5]. From now on we refer to the entire class of *Aequorea*-derived fluorescent proteins as AFPs, whereas we use 'GFP' to denote green members of that family. The newest colour in the AFPs is 'CGFP', the Thr203Tyr mutant of CFP (where Thr is threonine and Tyr is tyrosine). CGFP has an excitation and emission wavelength that is intermediate between CFP and EGFP[2]. Despite its dimness and broad excitation and emission peaks, the remarkably pH-resistant CGFP might find a use in the labelling of acidic organelles. First-generation YFPs such as GFP–Ser65Gly/Ser72Ala/Thr203Tyr[6] (where Ser is serine, Gly is glycine and Ala is alanine) were notorious for their sensitivity to pH, chloride fluctuations and PHOTOBLEACHING. A second-generation enhanced YFP (YFP–Val68Leu/Gln69Lys; where Val is valine, Leu is leucine, Gln is glutamine and Lys is lysine) slightly improved acid resistance, but only in third-generation derivatives named 'Citrine'[3] (YFP–Val68Leu/Gln69Met; where Met is methionine) and 'Venus'[4] (YFP–Phe46Leu/Phe64Leu/Met153Thr/Val163Ala/Ser175Gly; where

AFP

Box 1 | Considerations in designing and constructing AFP-based fluorescent reporters

Choice of *Aequorea* fluorescent protein (AFP) variant(s)

- For intermolecular fluorescence resonance energy transfer (FRET)-based reporters (FIG. 5a), non-oligomerizing cyan fluorescent protein (CFP) and yellow fluorescent protein (YFP) variants that incorporate the Ala206Lys mutation (where Ala is alanine and Lys is lysine) are strongly recommended.
- For intramolecular FRET-based reporters (FIG. 5b), CFP should be paired with one of the latest generation YFPs such as Citrine or Venus. Further improvements to monomeric red fluorescent protein (mRFP) should provide a new FRET partner for GFP.
- For single-fluorophore conformation-sensitive reporters (FIG. 4), insertion at Tyr145 (where Tyr is tyrosine), or the use of a circularly permuted AFP or YFP is recommended.

Spectral response

- The dynamic response range of the reporter must span physiologically relevant conditions.
- A ratiometric response, as obtained from a FRET reporter, is preferable to a simple increase in fluorescence intensity.
- For most reporter constructs, optimization of polypeptide linkers between components of the reporter is crucial for the success of the construct or for maximizing the fluorescent response.

Spatio-temporal resolution

- Spatio-temporal resolution will be lost with a freely diffusing cytosolic reporter that responds slowly relative to the timescale of diffusion.
- Genetic targeting to a compartment or anchoring to a subcellular structure can improve spatio-temporal resolution.

Perturbation of intracellular conditions

- Depending on the design strategy and the expression level, the introduction of the reporter might perturb the cellular component of interest or be toxic.

Specificity

- The reporter must respond to only the stimulus of interest.
- Genetic targeting can help increase biological specificity.

Versatile molecular construction

- Consideration of the available structural data can provide a rational basis for reporter construction.
- Ideally, the design strategy should be transferable to other members of the same protein family and structural homologues.

Phe is phenylalanine) has the chloride sensitivity been eliminated and the sensitivity to pH changes and photobleaching improved greatly. Specifically, Citrine remains 50% fluorescent at the lowest pH (5.7) that has been reported so far for a YFP and shows a twofold increase in photostability relative to YFP–Val68Leu/Gln69Lys, whereas Venus is the brightest and fastest maturing (with reference to the development of fluorescence) YFP so far. Unfortunately, simply transferring the crucial Gln69Met mutation of Citrine to Venus did not confer improved photostability[4] on Venus, and so there is not yet a single YFP that is superior for all applications.

Fluorescent 'highlighters'. Fluorescent proteins that can be modulated photochemically are molecular 'highlighters' that allow specific organelles or protein subpopulations to be marked by brief, localized, intense illumination and then tracked in space and time. Early versions showed only a modest contrast[7] or could only be used under anaerobic conditions[8,9]. A new YFP mutant, 'PA–GFP' (GFP–Val163Ala/Thr203His; where His is histidine) undergoes up to a 100-fold increase in fluorescence (excitation at 488 nm) when illuminated at 413 nm[10]. An even more spectacular fluorescent protein is 'Kaede' from the stony coral *Trachyphyllia geoffroyi*, which can be converted from a green to a stable red fluorescent protein by irradiation with 350–400-nm light[11]. This colour change corresponds to a 2,000-fold increase in the red to green ratio and allows both the irradiated and unirradiated species to be visualized separately with excitation wavelengths (475 and 550 nm) that do not cause any further colour change. At present, Kaede exists as a tetramer; if it can be mutated to a monomer, it should match or surpass PA–GFP in its ability to reveal the dynamic trafficking of fusion proteins.

In addition to the photoenhancement of fluorescence described above, AFP fusions find use in fluorescence recovery after photobleaching (FRAP), fluorescence loss in photobleaching (FLIP), and fluorescence correlation spectroscopy (FCS) — other powerful techniques that can assess protein trafficking and mobility in live cells (for a review, see REF. 12).

Limiting monomer–monomer interactions. The only instance when the weak tendency of AFPs to dimerize has been documented to cause artefacts or dysfunction was in the clustering of lipid-anchored AFPs on the plasma membrane[13]. At high concentrations, AFPs might interact with each other, which results in a false-positive interaction as determined by

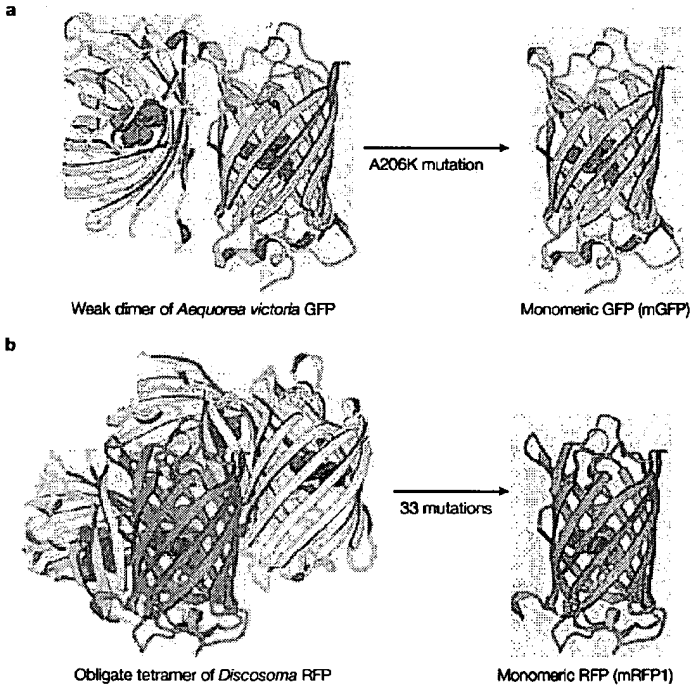

Figure 1 | **Recent advances in fluorescent proteins. a** | Introduction of the A206K mutant in *Aequorea* fluorescent proteins (AFPs) suppresses their tendency to dimerize. **b** | Several rounds of directed evolution and a total of 33 mutations were required to rescue the red fluorescence of a *Discosoma* red fluorescent protein (RFP) (DsRed or drFP583)-derived monomer following the introduction of interface-disrupting mutations.

FLUORESCENCE RESONANCE ENERGY TRANSFER (FRET). The non-radiative transfer of energy from a donor fluorophore to an acceptor fluorophore that is typically < 80 Å away. FRET will only occur between fluorophores in which the emission spectrum of the donor has a significant overlap with the excitation of the acceptor.

QUANTUM YIELD The probability of luminescence occurring in given conditions — expressed by the ratio of the number of photons that are emitted by the luminescing species to the number of photons that are absorbed.

FLUORESCENCE RESONANCE ENERGY TRANSFER (FRET). This tendency to dimerize[14,15] can be reduced greatly or eliminated by mutating the hydrophobic amino acids that are in the dimerization interface to positively charged residues[13]. In AFPs, the effectiveness of these mutations increases in the order Phe223Arg < Leu221Lys < Ala206Lys (where Arg is arginine; FIG. 1a). It would now seem prudent to routinely use non-dimerizing mutants such as Ala206Lys when testing protein–protein interactions, or when AFP fusion proteins seem to be causing mis-targeting or dysfunction[13].

Long-wavelength red fluorescent proteins. Long-wavelength fluorescent proteins have long been sought for multicolour protein-tracking applications and for the construction of improved FRET-based reporters. Red fluorescence should provide greater tissue penetration and better spectral separation from cellular autofluorescence than either yellow or green fluorescence. The first red fluorescent protein (RFP) to be discovered was isolated from a coral of the *Discosoma* genus (this RFP is known as DsRed or drFP583)[16] and was received with much excitement, but its use has been limited severely by a number of problems. The DsRed protein requires incubation at 37°C for more than 30 h for the red fluorescence to reach a steady-state level, and a significant fraction of the protein retains the green fluorescent 490-nm excitation peak that is associated with its 'GFP-like' intermediate. In addition, DsRed is an obligate tetramer that will almost certainly tetramerize any cellular protein to which it is fused[17,18]. If the fusion partner is a monomeric protein, tetramerization might not necessarily be detrimental, but if the partner has any tendency to oligomerize by itself, gross aggregation and precipitation of the fusion is likely. If aggregation does occur, one strategy that has proven successful for both hexameric connexin-43 (REF. 19) and dimeric thymidine kinase[20] fused to DsRed, is to co-express either the unfused or EGFP-fused target protein, but this approach requires the titration of co-expression levels and dilution of the desired red signal.

A more universal solution to the problem of oligomerization is to re-engineer the RFP using a combination of targeted and random mutagenesis to minimize the oligomerization and other limitations of wild-type DsRed[21–25]. The original commercially available form of DsRed (known as DsRed1), which incorporated mammalian codon-usage preferences, was replaced by DsRed2, which showed a 2–3-fold improvement in the speed of fluorescence maturation at 37°C and a diminished 475-nm excitation peak[22,26]. DsRed2 has, in turn, been effectively superseded by T1, which reaches its full red fluorescence within tens of minutes[23]. T1 is now commercially available as DsRed-Express (Clontech, Palo Alto, USA). The first effectively non-oligomerizing RFPs came with the development of red fluorescent tandem dimers, in which two dimer-forming subunits are concatenated with a spacer that allows them to satisfy their crucial dimer interactions through intramolecular contacts[24,27]. The most recent advance is the engineering of a completely monomeric DsRed variant (mRFP1) that matures quickly, has no residual green fluorescence and excitation and emission wavelengths that are about 25 nm longer than the previous DsRed variants[24] (FIG. 1b). At present, mRFP1 is probably the best starting point for the construction of red fluorescent fusion proteins, even though it sacrifices some QUANTUM YIELD and photostability relative to the tandem dimer that is derived from DsRed (REF. 24).

Finding more fluorescent proteins. The search for new fluorescent proteins in coelenterate marine organisms has resulted in the discovery and cloning of approximately 30 distinct fluorescent proteins, although all but a handful of these remain minimally characterized[28,29]. Several of these proteins that deserve a special mention include: the dimeric *Renilla mulleri* GFP, with its exceptionally narrow excitation (498 nm) and emission (509 nm) peaks[30]; the DsRed homologues asFP595 (REF. 31) from *Anemonia sulcata* and dsFP593 (REF. 32) from *Discosoma*, which were engineered for improved red fluorescence at 595 nm and 616 nm respectively; the dimeric but dim HcRed from *Heteractis crispa*, which was derived from a tetrameric non-fluorescent chromoprotein and emits at 618 nm[26,33]; and finally eqFP611 from *Entacmaea quadricolor*, a tetrameric red fluorescent protein that emits at 611 nm and that can be dissociated to monomers at a high dilution[34].

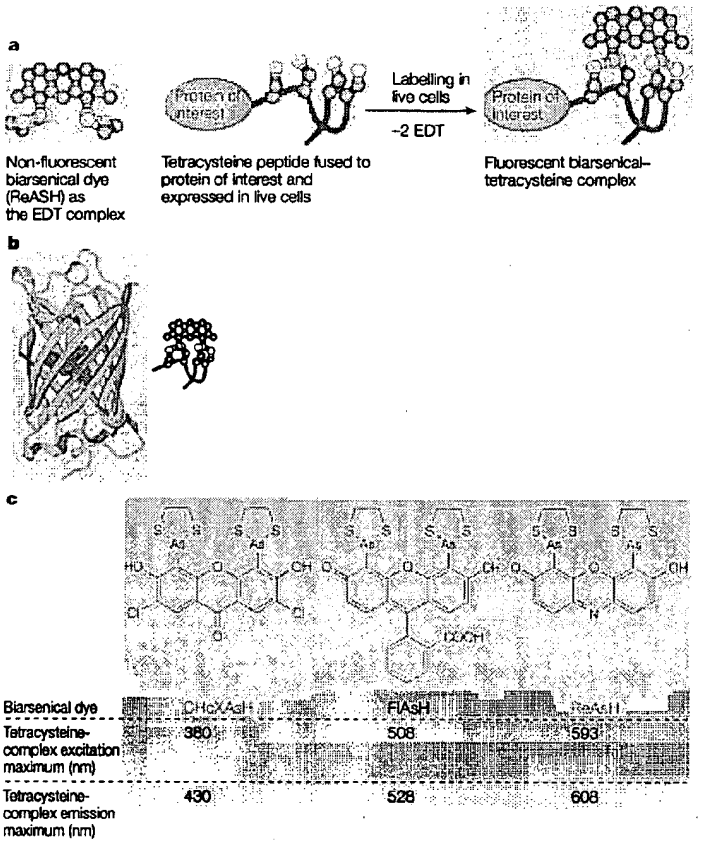

Figure 2 | **The biarsenical–tetracysteine system. a** | A non-fluorescent membrane-permeable biarsenical dye (ReAsH shown) forms specifically a fluorescent covalent complex with any intracellular protein to which a short tetracysteine-containing peptide (CCPGCC) has been genetically fused. The small size of the biarsenical dyes might be advantageous in those cases where a bulky *Aequorea* fluorescent protein (AFP) fusion disrupts normal protein function. The arsenical antidote ethanedithiol (EDT) is used to minimize the toxicity of any unbound biarsenical-dye. **b** | A comparison of the to-scale images of the green fluorescent protein (GFP) and biarsenical–tetracysteine complex. **c** | Fluorescent biarsenical labels that span the visible spectrum have been synthesized.

Recent advances in small molecule probes. Although GFP and its variants are extremely useful for tracking the expression and localization of proteins in cells, small-molecule probes with less steric bulk, faster rates of labelling and the ability to provide readouts in addition to, or other than, fluorescence are desirable.

The biarsenical–tetracysteine system. A promising alternative to GFP is the biarsenical–tetracysteine system (FIG. 2a) in which a recombinant protein that is expressed in a living cell is site-specifically labelled with a membrane-permeable biarsenical dye, which can be blue, green or red fluorescent (FIG. 2c)[35–37]. The specificity for the labelling reaction is provided by a small tetracysteine motif (at present, CCPGCC is the preferred motif) — the nucleic acid sequence of which can be fused to the gene encoding the protein of interest. The biarsenical dye and tetracysteine motif form a covalent complex in which each of the dye's arsenic atoms cooperatively binds a pair of cysteines. Toxicity is minimized by the administration of 1,2-dithiols, for example ethanedithiol (EDT) — antidotes that protect endogenous pairs of cysteines and keep the dyes largely non-fluorescent until they find their ultimate tetracysteine targets. Nevertheless, at present, background staining keeps the sensitivity and the detection limit of this method to an order of magnitude or so worse than those of GFP. The other main limitation of this method is that the target cysteines must be in their reduced form before they can bind the biarsenical dye. Although this will generally be true for cysteine residues in the reducing environment of the cytosol or nucleus, cysteines that are in the lumen of the secretory pathway or outside cells tend to oxidize spontaneously and they can only be labelled if acutely reduced.

Of the biarsenical dyes already characterized[37] (FIG. 2c), a resorufin-based red label (ReAsH) is particularly useful as it can be used for both fluorescence and electron microscopy (EM). Under intense illumination in fixed samples, ReAsH catalytically generates singlet oxygen, which oxidizes diaminobenzidine into a highly localized polymer, which is readily stained by osmium tetroxide for EM contrast. So tetracysteine tags constitute genetically targetable tags for EM that show catalytic amplification, but do not require the diffusion of large antibody molecules into fixed or frozen tissue[38].

Furthermore, sequential labelling with different biarsenical dyes can indicate the age of protein molecules. The tetracysteine motifs are labelled rapidly and saturably with one colour of a membrane-permeant biarsenical dye, such as green FlAsH (FIG. 2c), then any free dye is washed out and the live cells allowed to synthesize fresh unlabelled copies of the same tagged protein. A final exposure of the protein to a biarsenical dye of a different colour, such as red ReAsH, labels only the newly synthesized copies. This approach was used to study the life cycle of connexin-43 as it was trafficked into and out of gap junctions (FIG. 3). Newly synthesized connexins (red) enter the gap junctional plaques from their outer edges while older molecules (green) are removed by endocytosis from the plaque centres. Varying the order and timing of FlAsH versus ReAsH administration can control whether ReAsH labels exocytic vesicles that carry new connexin molecules or endocytic compartments that contain old molecules, and thereby enables each population to be visualized separately by EM[38]. The conclusion that connexins move progressively from the periphery to the centre of gap junctions agrees with the work of Lauf *et al.*[39], who photobleached gap junctions that contained GFP-tagged connexins and observed that newly synthesized connexins formed a thin fluorescent halo that thickened with time.

So, the biarsenical sequential labelling technique and photochemical marking overlap somewhat in their areas of applicability, and they can reach concordant conclusions. The biarsenical technique is unique in the small size of the tag and the ability to give EM as well as fluorescence images; the photochemically sensitive fluorescent proteins have better time-resolution, lower

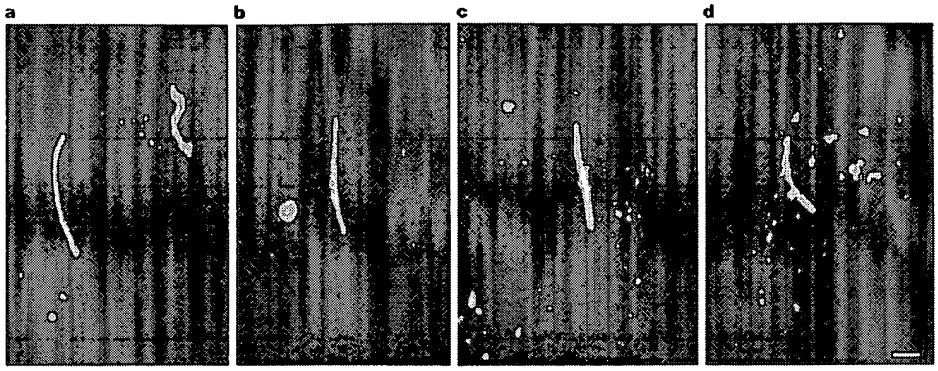

Figure 3 | **Multicolour pulse–chase biarsenical staining of gap junctions.** FlAsH and ReAsH were used to label two temporally separated pools of connexin-43 that had been fused to a tetracysteine-containing peptide (Cx43–4Cys) and then junctional plaque renewal was recorded over time[38]. HeLa cells that were expressing Cx43–4Cys were stained with FlAsH, incubated for 4 h (**a**,**b**) or 8 h (**c**,**d**), and then stained with ReAsH. Panels **a** to **d** show junctional plaques at different stages of renewal, as indicated by the different ratios of FlAsH (green) and ReAsH (red) stains. The green central zones diminish as the time interval between FlAsH and ReAsH staining increases from 4 to 8 h. Scale bar represents 1 μm. Adapted with permission from REF. 38 © 2002 American Association for the Advancement of Science.

background levels and can be marked with geometrically defined spatial patterns.

Antibody–hapten labelling. An alternative fluorescent dye-based labelling system consists of a single chain antibody which binds specifically to membrane-permeant fluorescent conjugates of its phenyloxazolinone hapten[40]. At present, because the antibody does not fold well in reducing environments, this system is best suited for use in secretory compartments and so has a complementary preference to the biarsenical–tetracysteine system. Ultimately it would be desirable to increase the affinity of the antibodies for the hapten (now an approximately 5 nM dissociation constant), and the extent to which antibody binding enhances fluorescence (~5-fold at present).

Avidin–biotin labelling. Another receptor–ligand pair that works best in the secretory compartment is the avidin–biotin pair, which is extremely popular for use *in vitro* and in histology, but has been surprisingly neglected in live cells. Chicken avidin that is expressed recombinantly in different compartments of the secretory compartment can trap biotin conjugates of fluoresceins of various pK_a values for the measurement of the pH values of those compartments, which enables the mechanism of pH regulation to be studied[41–43]. The availability of biotin conjugates and their extremely high affinity for avidin are advantages of this approach. Limitations include the tightly tetrameric nature of avidin and the essential role for biotin in the cytosol and mitochondria, such that avidin in these compartments is either toxic or biotin-saturated[44].

Phycobiliproteins. Bilin-containing proteins are important antennae for photosynthesis in cyanobacteria and photoreceptor signalling in green plants. Because they can absorb light at wavelengths that extend to the infrared, significant efforts have been made to develop biliproteins as fluorescent fusion tags — this is despite their natural oligomeric structure and their requirement for exogenous bilin cofactors or co-expression of the additional enzymes that are required for biosynthesis of the cofactor. Heterologous expression of the cyanobacterial truncated phytochrome[45], C-phycocyanin[46] and phycoerythrocyanin[47] has been achieved. The most promising class of these PHYCOBILIPROTEINS is the homodimeric phytofluors[48], which have excellent spectral properties, can be engineered as monomers and would require the co-expression of as few as three proteins[45].

Uroporphyrinogen III methylation. Another fluorescent reporter system, which seems to have been overshadowed by DsRed, is the recombinant uroporphyrinogen III methyltransferase gene (*cobA*)[49]. The cobA reporter catalyses the trimethylation of endogenous uroporphyrinogen III to generate a fluorescent small-molecule product that accumulates intracellularly. Although the cobA reporter system is not amenable to either subcellular targeting or the construction of fusion proteins, there could be certain cases in which its unique combination of a red fluorescent emission, independence from any exogenous cofactor and catalytic signal amplification will find a use.

Passive applications of fluorescent proteins

For most fluorescence imaging applications, the fluorescent label is a biologically inert participant that is used merely as a visible marker. By the very nature of their barrel-like structures (FIG. 1), which effectively shield the CHROMOPHORE from the external environment, AFPs are well suited to these more passive applications. Typical passive uses of AFPs include monitoring the appearance, degradation, location or translocation of appropriate partner proteins to which they are fused.

pK_a
The pH at which a molecule, or a particular site within a molecule, carries an ionizable H^+ 50% of the time.

Proteins from blue-green algae and red algae that exhibit intense fluorescence owing to the presence of multiple bilin chromophores that are covalently attached to the protein.

The core portion of a molecule that is directly responsible for absorbing photons. Chromophores usually contain alternating single and double bonds.

Table 1 | **Translocating fluorescent probes**

Domains	Source proteins	Target molecules	References
PH domain	For example, Akt, ARNO, GRP1	3′ phosphoinositides including PtdIns(3,4,5)P_3 and PtdIns(3,4)P_2	55–59
PH domain	PLC	PtdIns(4,5)P_2 and InsP_3	60,61
C1 domain	PKC	DAG	62
C2 domain	PKC	Ca^{2+}	63,64
PA domain	Raf-1	PA	65

Akt, a serine/threonine kinase, also known as protein kinase B; C1 and C2, conserved domains 1 and 2 from protein kinase C; ARNO, ADP-ribosylation factor nucleotide-binding-site opener; C1, C homology-1; C2, C homology-2; DAG, Diacylglycerol; GRP1, general receptor for 3-phosphoinositides; InsP_3, inositol 1,4,5-trisphosphate; PA, phosphatidic acid; PH, pleckstrin-homology; PKC, protein kinase C; PLC, phospholipase C; PtdIns(3,4,5)P_3, phosphatidylinositol 3,4,5-triphosphate; PtdIns(4,5)P_2, phosphatidylinositol 4,5-biphosphate ; Raf 1, a serine/threonine kinase important in mitogen-activated signalling.

Fluorescence as a spatial marker

Perhaps the most popular application of fluorescent probes is to use fluorescence as a visible label to reveal either the static or dynamic spatial patterning of various cellular components. In 1995 it was still feasible to compile a nearly exhaustive list of AFP–fusion proteins[50], however, the number of published AFP–fusion proteins has since risen to many hundreds, if not thousands, and compilation of an updated list is far beyond the scope of this review.

Protein trap strategies. An interesting twist to the fluorescence imaging of intracellular localization is the identification of previously unknown protein targets on the basis of their pattern of localization[51]. In the so-called 'protein trap' strategies, a visual screen of cells that contain fusions of an AFP gene and a library of coding DNA sequences is used to identify cells that give rise to a pattern of interest. The DNA sequence that encodes the targeted fusion can then be cloned directly from the cell and the novel protein, which is presumably directing the localization, can be identified.

Fluorescent speckle microscopy. One particularly powerful technique for monitoring cytoskeletal dynamics is fluorescent speckle microscopy[52,53]. A fluorescently labelled protein is introduced into a cell at a very low level (~ 0.25%) relative to its endogenous counterpart, such that individual fluorescently labelled proteins can be detected with a sensitive imaging system. The dynamic assembly and disassembly of the actin cytoskeleton is shown by the 'flow' of the individual fluorescent speckles from regions of filament synthesis to regions of depolymerization. In order to get enough signal from a single protein it is necessary to either attach multiple small-molecule labels or to fuse the gene encoding the protein of interest to multiple AFP sequences[54].

Localizing the messenger. When fused to minimal protein domains that interact specifically with small-molecule messengers, AFPs can provide a straightforward readout of the cellular localization and transient production of such messengers[55–65]. For example, AFP that is fused to the pleckstrin-homology (PH) domain shows, through translocation from the general cytosol to the plasma membrane, the generation of 3′-phosphoinositides at the cell's leading edge on exposure to a chemoattractant[58,59]. Other messengers, such as phosphatidic acid and diacylglycerol (DAG), have been detected by similar methods (TABLE 1). In one elegant study, the comparison of the kinetics of translocation of full-length protein kinase C (PKC) versus the individual DAG-binding C1 domain and the Ca^{2+}-binding C2 domain led to a model for a sequential activation of PKC through a temporal coordination of the Ca^{2+} and DAG signals[64].

Localizing gene activity and transcripts. RNA localization can be visualized in live cells through fluorescence *in vivo* hybridization (FIVH)[66] or fusion of AFP to an RNA-binding protein or domain[67–70]. Using the latter approach, researchers have visualized the movement of endogenous bicoid messenger RNA during *Drosophila melanogaster* oogenesis through the use of AFP fused to Exu, a protein which accompanies bicoid mRNA during transport[69]. In a separate study, imaging of live neurons that were transfected with GFP-fused zipcode binding protein 1 (ZBP1) showed fast, bidirectional movements of granules in neurites, which can be inhibited by antisense oligonucleotides to the actin mRNA *zipcode* sequence[70]. Visualization of gene activity and changes in chromatin structure during transcription has also been achieved by creating large tandem arrays of DNA sequences (such as the *lac* operator or mouse mammary tumour virus promoter) that can be recognized with AFP-tagged DNA-binding proteins such as *lac* repressor or glucocorticoid receptor[71–74].

Fluorescence as a temporal marker

Analysing gene expression. AFPs are a favourable alternative to β-galactosidase (*lacZ*) as a marker of gene expression in tissue sections and transgenic organisms, because AFPs are self-sufficient and form their own chromophores[75]. The main disadvantage of AFP relative to enzymatic reporter systems is the absence of signal amplification. Whereas AFP is limited to a single FLUOROPHORE for each protein, a single copy of β-galactosidase, luciferase or β-lactamase[76] will catalyze the turnover of multiple substrate molecules, which allows much lower levels of gene expression to be detected. One approach to overcome this drawback is to target the AFP to a defined subcompartment of the cell and thereby use local contrast to distinguish its fluorescence from background autofluorescence.

FLUOROPHORE
A chromophore that can re-emit photons.

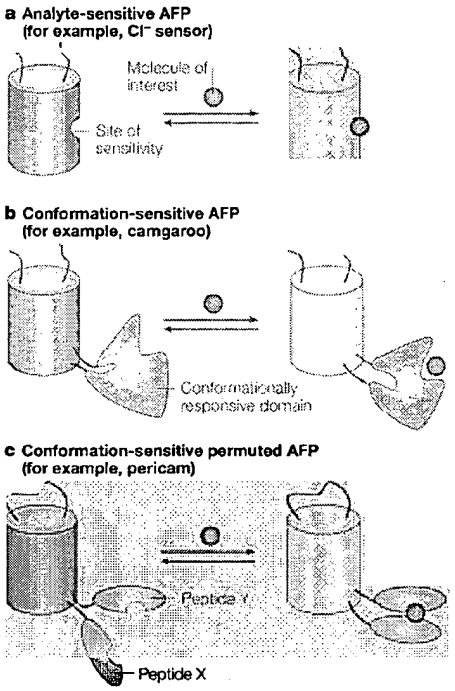

Figure 4 | **Biochemical modulation of AFP fluorescence.** **a** | *Aequorea* fluorescent protein (AFP) can be engineered to be directly sensitive to a small molecule of interest. **b** | Insertion of a conformationally responsive domain into AFP can result in a chimaera in which fluorescence is modulated by the conformational change. **c** | Alternatively, interacting proteins (or peptides) can be fused to the amino and carboxyl termini of circularly permuted AFP.

Optimizing turnover. Increasingly sophisticated reporters have been developed to monitor the temporal patterns of gene expression and protein dynamics. A limitation of AFP and similar passive markers is that the new protein cannot be distinguished from the old protein, as AFP remains fluorescent until it is degraded. Degradation can be accelerated by the fusion of AFP to degradation domains such as that of the mouse ornithine decarboxylase[77], thereby destabilizing the fluorescent protein such that it is turned over with a half-life of 2 h or less. These destabilized AFP variants minimize the accumulation of the background fluorescence that is generated by leaky, non-induced basal-level expression, which enhances their use as transcriptional reporters, albeit at the inherent cost of lower sensitivity — that is, a higher level of transcription and translation are required to produce a given level of fluorescence.

A DsRed fluorescent timer. A 'fluorescent timer' version of DsRed has been developed as a temporal marker[78]. The variant changes from green to red fluorescent over a period of ~24 h as the 'GFP-like' intermediate that accumulates is converted to the final red species owing to a further oxidative modification of the chromophore. The temporal history of the promoter activation is therefore reflected in the ratio between green and red fluorescence. Because the timescale of the fluorescent change is fixed and the resolution is restricted to several hours, this system will probably be most useful for the analysis of developmental control genes[78] in systems where the photochemically triggered green-to-red conversion of Kaede[11] or pulse–chase labelling of tetracysteine motifs[38], which were discussed previously, cannot be applied.

Analysing protein dynamics. Through the use of innovative fusion constructs, AFPs can report the temporal dynamics of cellular processes other than promoter activation. For example, the accumulation and degradation of an AFP-based substrate has been used for the quantification of ubiquitin–proteasome-dependent proteolysis in living cells[79]. Another tactic, which has found a use in the monitoring of vesicular traffic and sorting in the secretory pathway, is based on temperature-sensitive GFP mutants that fold and mature correctly only at temperatures that are non-permissive for sorting events. By growing cells at such temperatures, a cohort of fluorescently tagged proteins can accumulate in the *trans*-Golgi network. On raising the temperature, both to allow sorting and to prevent folding of the newly synthesized GFPs, the fate of the fluorescent 'bolus' can be monitored[80]. This pulse–chase-type approach has been used recently to visualize specifically the dynamics of immature secretory granules in a much larger pool of mature secretory granules[81]. So the age and fate of protein fusions can be monitored by spontaneously slow-maturing fluorescent proteins, temperature- or illumination-sensitive fluorescent proteins or pulse–chase labelling by biarsenical ligands, all of which have their own advantages and drawbacks.

Genetically encoded biochemical sensors

In the more active applications of fluorescent proteins that are described below, biochemical parameters such as metabolite concentrations, enzyme activity, or protein–protein interactions can be detected by their effects on the fluorescence properties of the designed indicators. Such indicators can be further divided into molecules with single chromophores (FIG. 4a–c) versus composites in which the emission intensity is dependent on the energy transfer between two chromophores (FIG. 5a,b).

Modulation of fluorescent protein spectra

Exploiting pH and halide-sensitive fluorescent proteins. In general, the fluorescence of AFPs is quenched reversibly by moderate acidification. This intrinsic pH sensitivity varies between different mutants and can be exploited to measure the ambient pH[82–84]. Both intensity-modulated and ratiometric pH-sensitive variants of GFP have been engineered and fused to a vesicle membrane protein to monitor vesicle exocytosis and recycling. These 'synapto-pHluorins' report synaptic neurotransmitter secretion by detecting the abrupt pH change that occurs when the acidic interior of the

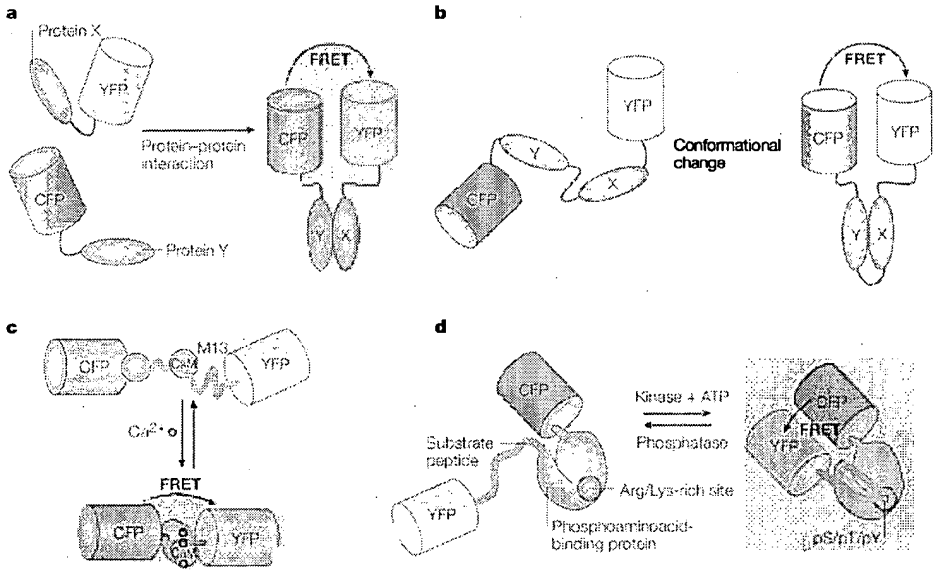

Figure 5 | **The general design of FRET-based fluorescent probes. a** | An intermolecular fluorescence resonance energy transfer (FRET)-based probe consists of two different proteins (X and Y) that are labelled with cyan fluorescent protein (CFP) and yellow fluorescent protein (YFP), respectively, which interact and bring the fluorophores into close proximity, thereby increasing the FRET efficiency. **b** | An intramolecular FRET-based probe consists of either a cleavable linker or a conformationally responsive region sandwiched between a FRET pair. **c** | Cameleon is an intramolecular FRET-based probe that is used to measure intracellular Ca^{2+}. **d** | Intramolecular phosphorylation-sensitive FRET probes have been constructed with specificities for various different kinases. Arg, arginine; CaM, calmodulin; Lys, lysine; pS, phosphoserine; pT, phosphothreonine; pY, phosphotyrosine. Figure 5, part **c** is reprinted with permission from REF. 105 *Nature* © (1997) Macmillan Magazines Ltd. Figure 5, part **d** is reproduced with permission from REFS 116,118 © 2002, National Academy of Sciences.

vesicle (pH ~5) is exposed to the outside of the cell (pH ~7) on fusion to the plasma membrane[84]. Some YFPs have particularly high pK_as in the range of 7 to 8, which makes them very useful for monitoring the pH of the cytosol and the mitochondrial matrix[45]. These same YFPs are quenched by halide ions, which bind selectively in the order $F^- > I^- > Cl^- > Br^-$ and raise the pK_a, which simulates acidification[86,87]. The halide-sensitive YFPs have been used in live cells to monitor Cl^- fluxes such as those mediated by the cystic fibrosis transmembrane conductance regulator (CFTR)[88]. Although the above indicators only change the intensity of fluorescence, examples of wavelength-shifting pH[89] and halide[90] indicators are also known. The responsiveness of YFPs to both protons and halides means that care has to be taken to disentangle the two perturbations. Sensitivity to pH and Cl^- can be a significant annoyance in applications where the YFP is to only be maximally fluorescent and inert (as in the passive applications discussed above). Fortunately, alternative YFPs with reduced pK_as, no halide sensitivity and increased brightness and photostability are now available[3,4].

Engineering fluorescent proteins to be sensitive to other parameters. The fluorescence of fluorescent proteins can be made directly sensitive to other signals by the introduction of specific mutations into the well-defined chromophore or barrel structure. A blue fluorescent protein (BFP) has been engineered, by the introduction of point mutations, to bind Zn^{2+} directly on the chromophore[91], but the modest fluorescence enhancement (twofold), low Zn^{2+} affinity (50 μM K_d) and slow association rate ($t_{1/2}$ > 4 h) would need considerable improvement to become biologically useful. YFPs[92] and GFPs (G. T. Hanson, R. Aggeler, R. A. Capaldi, and S. J. Remington, unpublished observations) that are responsive to thiol-disulphide redox potentials have been engineered by placing two cysteine residues on adjacent β-strands so that they can form a reversible intramolecular disulphide bond. Such oxidation reduces the fluorescence of the YFP-based sensor by 2.2-fold[92], whereas it shifts the excitation maxima of the GFP-based sensors from 475–490 nm to 400 nm, which alters the excitation ratio by as much as 6–8-fold. Such indicators hold great promise, because, at present, the redox potentials of different compartments of cells are difficult to measure, but they are probably very important, heterogeneous and at least somewhat dynamic.

Most other biochemical parameters would require binding or sensing sites that are more complex than those created by point mutations in AFPs. Conformationally responsive elements, which range from short peptide motifs to full-length proteins, can be inserted into AFPs. The best-characterized example is the insertion of calmodulin (CaM) in place of Tyr145 of YFP, which

results in Ca^{2+} sensors (known as camgaroos) that increase fluorescence sevenfold on binding of Ca^{2+} (REFS 3,93). Camgaroos have proved to be useful for imaging Ca^{2+} inside mitochondria[94] and in MUSHROOM BODIES in the brain of *Drosophila*[95].

An important topological variation of this is to insert an AFP inside a conformationally responsive protein or pair of protein domains. An early example was a voltage sensor that consisted of AFP inserted into a non-conducting mutant of the Shaker K^+ channel[96]. More recently a smaller but faster response has been obtained by inserting wild-type GFP into a sodium channel[97]. Even larger responses might be obtained by inserting a circularly permuted AFP (cpAFP) rather than wild-type GFP[3,93]. In a cpAFP, the original amino and carboxyl termini are joined by a flexible linker, and new amino and carboxyl termini are introduced at one of several possible locations near the chromophore. Such permutation increases the flexibility and optical responsiveness to stresses that are applied on the new termini. Insertion of circularly permuted GFP (cpGFP) between CaM and M13 (a peptide which binds calmodulin in a Ca^{2+}-dependent fashion) yields Ca^{2+} indicators that are known as GCaMP[98] or pericams[99]. The inclusion of M13 increases the apparent Ca^{2+} affinity of the CaM by allowing the formation of ternary complexes, so that these molecules are more sensitive than camgaroos to small elevations in physiological levels of Ca^{2+}. Some pericam variants shift their excitation wavelengths on binding of Ca^{2+}, as opposed to just increasing fluorescence, which thereby enables ratiometric observation[99].

Intramolecular FRET-based indicators

FRET is a quantum-mechanical phenomenon that occurs when two fluorophores are in molecular proximity of each other (< 80 Å apart) (BOX 2). The emission spectrum of the donor fluorophore should overlap the excitation spectrum of the acceptor fluorophore, but both excitation spectra should be well enough separated to allow independent excitation. When the stoichiometry of the donor and the acceptor is fixed, as it is when they are fused in a single polypeptide chain, then the experimentally most convenient readout of FRET is the ratio of acceptor to donor fluorescence. Many reporters that are designed on the basis of intramolecular FRET changes (FIG. 5b) have been developed for measuring biochemical events in cells. Early applications used BFP as the donor and GFP as the acceptor, but the dimness and ability of BFP to be bleached soon led to its replacement by CFP, whereupon GFP had to be replaced by YFP to maintain spectral separation. When monomeric RFPs have been optimized sufficiently, GFP–RFP will probably become the next donor–acceptor pairing of choice.

Indicators of protease activity. The earliest FRET reporters consisted of BFP and GFP fused together with a protease-sensitive linker. Proteolysis disrupts FRET by separating the donor and acceptor units[100,101]. More recent examples have used CFP and YFP to measure caspase activity during apoptosis[102,103], which includes all-or-none activation at the single-cell level[104].

Indicators for measuring changes in calcium. Genetically encoded Ca^{2+} indicators, which are known as cameleons, were constructed by sandwiching CaM, a peptide linker and M13 between CFP and YFP[3,105–107] (FIG. 5c). Increased levels of intracellular Ca^{2+} switches on the affinity of CaM for the adjacent M13 sequence, which results in a change in orientation or distance between the two fluorescent proteins and a large increase in FRET. The replacement of glutamate by glutamine residues in the Ca^{2+}-binding sites tunes the effective affinity for Ca^{2+}. The replacement of M13 by a peptide that is derived from CaM-dependent kinase kinase produces a cameleon analogue with a larger, although somewhat slower, response than the traditional cameleons[108]. Levels of free intracellular CaM–Ca^{2+} complex can be sensed by reporters in which the donor and acceptor are connected by just a CaM-binding peptide[109,110], but in this case the binding of CaM straightens the peptide linker and so decreases FRET.

Indicators for other cellular parameters. Over the past few years, this principle of indicator design has been applied to visualize the behaviour of many other signalling molecules and proteins in cells. For example, indicators for cGMP (using cGMP-dependent protein kinase)[111,112], Ras and Rap1 activity[113], and Ran activity[114] have been constructed and applied to the study of a range of cell biological phenomena.

Reporters for the activity of tyrosine kinases[115–117] and serine/threonine kinases[118] have been made by sandwiching a substrate peptide for the kinase of interest and a phosphoaminoacid-binding domain, such as Src-homology-2 (SH2) or 14-3-3, between CFP and YFP (FIG. 5d). Phosphorylation of the substrate peptide induces the formation of an intramolecular complex with the neighbouring phosphoaminoacid-binding domain, which changes the FRET. This generic concept has been adapted to create probes for Abl, Src, the epidermal growth factor (EGF) receptor, insulin receptor, protein kinase A (PKA), and PKC, (J. D. Violin, J. Z., R. Y. T., and A. C. Newton, unpublished observations) with many more underway. The FRET change is usually reversed by phosphatases, so the fluorescent substrates report continuously the balance between kinase and phosphatase activities, with time resolution in the order of a few seconds and a spatial resolution of micrometres — far better than conventional assays with radioactive phosphorus or phospho-specific antibodies. Even finer spatial discrimination is possible if the reporters are fused to specific components of scaffolding molecules. So phosphorylation kinetics can differ significantly between sites that are indistinguishable at the resolution of the light microscope[118].

A FRET-based reporter of membrane potential exemplifies a slightly different topology, in which the voltage sensor, a truncated potassium channel, is placed amino terminal to both the CFP and YFP[119]. Voltage-dependent twists of the S4 channel helix are proposed to rotate the CFP with respect to the YFP.

MUSHROOM BODIES
Two prominent bilaterally symmetrical structures in the fly brain that are crucial for olfactory learning and memory.

Intermolecular FRET-based indicators

Indicators for cyclic AMP. The first fluorescent indicator for intracellular cAMP consisted of the PKA holoenzyme, in which the catalytic and regulatory subunits were labelled with fluorescein and rhodamine, respectively, so that cAMP-induced dissociation of the holoenzyme disrupted FRET[120]. Replacement of the dyes by BFP and GFP made this system genetically encodable and eliminated the need for *in vitro* dye conjugation and microinjection[121]. Application of this probe (with CFP and YFP replacing BFP and GFP) in cardiac myocytes showed an unusual compartmentalization of cAMP[122], whereas cAMP diffused freely in other cell types such as neurons[123,124].

Detecting protein–protein interactions. Intermolecular FRET can be used in real-time to detect interactions between two protein partners (FIG. 5a). Transcription factor homo- and heterodimerization[125,126], G-protein dissociation[127] and many other interactions[128–134] have all been visualized in live cells through the attachment of donor and acceptor fluorophores to interacting protein partners.

Protein–protein interactions can also be imaged by protein complementation assays, in which the potential partner proteins are fused not to FRET donors and acceptors but to complementary fragments of GFP[135], YFP[136], or other fluorogenic reporters[137,138], the most recent of which is β-lactamase[139,140]. The interaction of the partner proteins allows the two fragments to reconstitute the fluorescence or enzymatic activity, which is analogous to yeast two-hybrid assays in which transcriptional activation is reconstituted. Protein complementation assays generally have a much lower background and a greater dynamic range than those of FRET. When the reconstituted protein is an enzyme, its ability to catalyse the turnover of several copies of a substrate provides useful amplification, but it sacrifices subcellular spatial resolution if the reaction product is diffusible. However, FRET is instantaneous, fully reversible (that is, it monitors dissociation as well as association), has a well-characterized dependence on distance (BOX 2) and orientation, does not require the partner proteins to touch each other and contributes no attraction or repulsion of its own, provided that non-dimerizing fluorescent proteins are chosen[13]. Protein complementation takes from minutes to hours for the fragments to fold, reversibility is absent or uncertain and the requirements on the conformation and affinity of the partner proteins are quantitatively ill-defined except that they must bring the two reporter fragments into the correct juxtaposition.

Notes of caution. When the FRET donor and acceptor are in two separate molecules rather than a fused chimaera, the involvement of mixed complexes between labelled and endogenous partners becomes a greater concern, and the ratio of donor to acceptor expression is no longer fixed. FRET can no longer be assessed by exciting the donor and measuring the ratio of emissions in the donor and acceptor bands. More sophisticated methods such as the mathematical processing of three images[141–144], measuring donor dequenching on photobleaching the acceptor[13,107,126,130], or FLUORESCENCE-LIFETIME IMAGING MICROSCOPY (FLIM; see below) are required to show and quantify FRET.

Intermolecular FRET can suffer from false negatives when the donor and acceptor fluorescent proteins are: perturbing the proteins to which they are fused; in close proximity but orientated unfortunately with respect to each other; too far away from each other even when their fusion partners are interacting. Concern over false negatives has probably been the main reason why intermolecular FRET has been used mainly to obtain higher spatio-temporal resolution on known interactions rather than to screen proteomes for unknown interactions. False positives could result from the weak affinity (K_d ~ 0.1 mM) of AFPs for each other, but the only known example is when CFP and YFP were anchored to the plasma membrane by fatty acyl anchors, in which case the confinement to a surface probably raised the effective concentration considerably[13]. After the dimerization was eliminated by the monomerizing mutations described above, correlation of FRET efficiency versus YFP density showed that in living cells acyl, but not prenyl, modifications promote clustering in lipid rafts on the cytosolic face of the plasma membrane[13].

Box 2 | FRET

Fluorescence resonance energy transfer (FRET) is a quantum mechanical phenomenon that occurs between a fluorescence donor and a fluorescence acceptor that are in molecular proximity of each other if the emission spectrum of the donor overlaps the excitation spectrum of the acceptor. Under these conditions, energy (E) is transferred non-radiatively from the donor to the acceptor with an efficiency defined by the equation, where r is the distance between the two fluorophores and R_0 (Förster distance) is the distance at which 50% energy transfer takes place (typically 20–60 Å).

$$E = \frac{R_0^6}{R_0^6 + r^6}$$

R_0 is dependent on the extent of spectral overlap between the donor and acceptor, the quantum yield of the donor and the relative orientation of the donor and acceptor.

Excitation of a donor fluorophore in a FRET pair leads to quenching of the donor emission and to an increased, sensitized, acceptor emission. Intensity-based FRET detection methods include monitoring the donor intensity with or without acceptor photobleaching, the sensitized acceptor emission or the ratio between the donor and acceptor intensity. Methods that are based on fluorescence-decay-kinetics include determining the rate of donor photobleaching, the decrease of donor fluorescence lifetime or the appearance of new components in the acceptor decay kinetics.

FLUORESCENCE-LIFETIME IMAGING MICROSCOPY (FLIM). An imaging technique in which the lifetime, rather than the intensity, of the fluorescent signal is measured. This approach can be used to measure FRET.

FLUORESCENCE-ACTIVATED CELL SORTING (FACS). A flow cytometry application in which live fluorescent cells are excited at a specific wavelength and then sorted into physically separated subpopulations on the basis of their fluorescence emission.

POSITRON EMISSION TOMOGRAPHY (PET). Positron emission tomography is an imaging technique that is used to detect decaying nuclides, such as ^{15}O, ^{13}N, ^{11}C, ^{18}F, ^{124}I and ^{94m}Tc.

MAGNETIC RESONANCE IMAGING The use of radio waves in the presence of a magnetic field to extract information from certain atomic nuclei (most commonly hydrogen, for example, in water). This technique is used to show certain types of tissue damage and the presence of tumours.

Fluorescence-lifetime imaging microscopy. Autophosphorylation of GFP-tagged PKC[145] or ErbB1 (REF. 146) has been measured by the FRET to Cy3-labelled phosphospecific antibodies, which were microinjected or applied to fixed cells and present in excess. When the acceptor is in such a large excess, FRET is best detected by the decrease in the lifetime of the donor's excited state using FLIM. FLIM and measurements of fluorescence depolarization allow the imaging of FRET between spectrally similar AFP molecules — that is, GFP–YFP or even GFP–GFP[147]. The main drawbacks of FLIM are that it sacrifices some sensitivity[134] and requires the assembly of expensive instrumentation.

Future directions

The applications of fluorescent probes will continue to expand and provide exciting new insights into the biology of living cells. Several relatively versatile reporter design strategies are now at our disposal (for example, translocation, camgaroo-, pericam- and cameleon-like strategies), but efforts to engineer new fluorophores and reporter classes must continue. For example, brighter and more red-shifted fluorescent proteins should improve the detection limits and *in vivo* applicability of AFP-based reporters. At present, all single AFP and FRET-based sensors rely on a gross structural reorganization or conformational change to produce a spectral readout. Many interesting intracellular process involve subtle conformational changes that are not amenable to the current classes of reporters, so that fluorescent protein variants with an increased sensitivity towards structural perturbations would be desirable. Another important consideration is that many of these fluorescent probes, in particular those for monitoring protein–protein interactions, function as surrogate cellular players. Visualization of their activities complement, but do not replace, measurements of endogenous components. Reporters that could assay endogenous biomolecules directly would therefore be very desirable.

Single-cell imaging with fluorescent reporters should allow the investigation of potentially interesting cell-to-cell variability that cannot be observed by the available methodologies that are based on cell population analysis[122]. Fluorescence is also an attractive readout for rapid, high-throughput approaches because of the availability of technologies such as multi-well plate readers, FLUORESCENCE-ACTIVATED CELL SORTING (FACS) and evanescent wave single-cell array technology (E-SCAT)[63].

Single-molecule spectroscopy is a young field that holds great promise. Single-molecule imaging in living cells allows the visualization of individual molecular interactions under physiological conditions and provides information that is difficult, and sometimes impossible, to obtain by conventional techniques[148]. Examples of single-molecule studies in living cells include investigations of EGF receptor dimerization[149], conformational changes in voltage-gated ion channels[150] and the mobility and aggregation of L-type Ca^{2+} channels in the plasma membrane[151].

For whole-body *in vivo* imaging, AFP has been used mainly as a visible localization marker[152] and a gene-expression marker[153]. Given the available wavelengths of excitation and emission, AFP imaging is still limited to surface structures (with a depth of penetration of approximately 1–2 mm) in experimental animals. A new generation of highly sensitive near infrared probes needs to be developed to complement existing non-optical probes for POSITRON EMISSION TOMOGRAPHY (PET) and MAGNETIC RESONANCE IMAGING (MRI).

1. Tsien, R. Y. The green fluorescent protein. *Annu. Rev. Biochem.* **67**, 509–544 (1998).
2. Sawano, A. & Miyawaki, A. Directed evolution of green fluorescent protein by a new versatile PCR strategy for site-directed and semi-random mutagenesis. *Nucleic Acids Res.* **28**, E78 (2000).
3. Griesbeck, O., Baird, G. S., Campbell, R. E., Zacharias, D. A. & Tsien, R. Y. Reducing the environmental sensitivity of yellow fluorescent protein. Mechanism and applications. *J. Biol. Chem.* **276**, 29188–29194 (2001).
4. Nagai, T. *et al.* A variant of yellow fluorescent protein with fast and efficient maturation for cell-biological applications. *Nature Biotechnol.* **20**, 87–90 (2002).
5. Scholz, O., Thiel, A., Hillen, W. & Niederweis, M. Quantitative analysis of gene expression with an improved green fluorescent protein. *Eur. J. Biochem.* **267**, 1565–1570 (2000).
6. Ormö, M. *et al.* Crystal structure of the *Aequorea victoria* green fluorescent protein. *Science* **273**, 1392–1395 (1996).
7. Yokoe, H. & Meyer, T. Spatial dynamics of GFP-tagged proteins investigated by local fluorescence enhancement. *Nature Biotechnol.* **14**, 1252–1256 (1996).
8. Sawin, K. E. & Nurse, P. Photoactivation of green fluorescent protein. *Curr. Biol.* **7**, R606–R607 (1997).
9. Elowitz, M. B., Surette, M. G., Wolf, P. E., Stock, J. & Leibler, S. Photoactivation turns green fluorescent protein red. *Curr. Biol.* **7**, 809–812 (1997).
10. Patterson, G. H. & Lippincott-Schwartz, J. A photoactivatable GFP for selective photolabeling of proteins and cells. *Science* **297**, 1873–1877 (2002).
11. Ando, R., Hama, H., Yamamoto-Hino, M., Mizuno, H. & Miyawaki, A. An optical marker based on the UV-induced green-to-red photoconversion of a fluorescent protein. *Proc. Natl Acad. Sci. USA* **99**, 12651–12656 (2002).

References 10 and 11 describe a pair of photoactivatable fluorescent proteins that can be used as fluorescent 'highlighters' to mark specific organelles or protein subpopulations.

12. Lippincott-Schwartz, J., Snapp, E. & Kenworthy, A. Studying protein dynamics in living cells. *Nature Rev. Mol. Cell Biol.* **2**, 444–456 (2001).
13. Zacharias, D. A., Violin, J. D., Newton, A. C. & Tsien, R. Y. Partitioning of lipid-modified monomeric GFPs into membrane microdomains of live cells. *Science* **296**, 913–916 (2002).
14. Ward, W. W., Prentice, H. J., Roth, A. F., Cody, C. W. & Reeves, S. C. Spectral perturbations of the *Aequorea* green-fluorescent protein. *Photochem. Photobiol.* **35**, 803–808 (1982).
15. Yang, F., Moss, L. G. & Phillips, G. N. Jr. The molecular structure of green fluorescent protein. *Nature Biotechnol.* **14**, 1246–1251 (1996).
16. Matz, M. V. *et al.* Fluorescent proteins from nonbioluminescent *Anthozoa* species. *Nature Biotechnol.* **17**, 969–973 (1999).
17. Tsien, R. Y. Rosy dawn for fluorescent proteins. *Nature Biotechnol.* **17**, 956–957 (1999).
18. Zacharias, D. A. Sticky caveats in an otherwise glowing report: oligomerizing fluorescent proteins and their use in cell biology. *Sci. STKE.* **2002**, PE23 (2002).
19. Lauf, U., Lopez, P. & Falk, M. M. Expression of fluorescently tagged connexins: a novel approach to rescue function of oligomeric DsRed-tagged proteins. *FEBS Lett.* **498**, 11–15 (2001).
20. Sating, A., Simm, A. & Rainov, N. Intracellular localization of Herpes simplex virus type 1 thymidine kinase fused to different fluorescent proteins depends on choice of fluorescent tag. *FEBS Lett.* **527**, 153 (2002).
21. Yanushevich, Y. G. *et al.* A strategy for the generation of non-aggregating mutants of *Anthozoa* fluorescent proteins. *FEBS Lett.* **511**, 11–14 (2002).
22. Terskikh, A. V., Fradkov, A. F., Zaraisky, A. G., Kajava, A. V. & Angres, B. Analysis of DsRed mutants: space around the fluorophore accelerates fluorescence development. *J. Biol. Chem.* **277**, 7633–7636 (2002).
23. Bevis, B. J. & Glick, B. S. Rapidly maturing variants of the *Discosoma* red fluorescent protein (DsRed). *Nature Biotechnol.* **20**, 83–87 (2002).
24. Campbell, R. E. *et al.* A monomeric red fluorescent protein. *Proc. Natl Acad. Sci. USA* **99**, 7877–7882 (2002).
This paper describes the directed evolution of a monomeric RFP that overcomes the problems associated with tetrameric DsRed.
25. Knop, M., Barr, F., Riedel, C. G., Heckel, T. & Reichel, C. Improved version of the red fluorescent protein (drFP583/DsRed/RFP). *BioTechniques* **33**, 592, 594, 596–598 (2002).
26. CLONTECH Laboratories Inc. *Living Colors User Manual Vol. II: Red Fluorescent Protein* 4 (Becton, Dickinson and Company, USA, 2002).
27. Fradkov, A. F. *et al.* Far-red fluorescent tag for protein labeling. *Biochem. J.* **368**, 17–21 (2002).
28. Labas, Y. A. *et al.* Diversity and evolution of the green fluorescent protein family. *Proc. Natl Acad. Sci. USA* **99**, 4256–4261 (2002).
29. Matz, M. V., Lukyanov, K. A. & Lukyanov, S. A. Family of the green fluorescent protein: journey to the end of the rainbow. *Bioessays* **24**, 953–959 (2002).
30. Peelle, B., Gururaja, T. L., Payan, D. G. & Anderson, D. C. Characterization and use of green fluorescent proteins from *Renilla mulleri* and *Ptilosarcus guernyi* for the human cell

display of functional peptides. *J. Protein Chem.* **20**, 507–519 (2001).
31. Lukyanov, K. A. *et al.* Natural animal coloration can be determined by a non-fluorescent GFP homolog. *J. Biol. Chem.* **275**, 25879–25882 (2000).
32. Fradkov, A. F. *et al.* Novel fluorescent protein from *Discosoma* coral and its mutants possesses a unique far-red fluorescence. *FEBS Lett.* **479**, 127–130 (2000).
33. Gurskaya, N. G. *et al.* GFP-like chromoproteins as a source of far-red fluorescent proteins. *FEBS Lett.* **507**, 16–20 (2001).
34. Wiedenmann, J. *et al.* A far-red fluorescent protein with fast maturation and reduced oligomerization tendency from *Entacmaea quadricolor* (*Anthozoa, Actinaria*). *Proc. Natl Acad. Sci. USA* **99**, 11646–11651 (2002).
35. Griffin, B. A., Adams, S. R. & Tsien, R. Y. Specific covalent labeling of recombinant protein molecules inside live cells. *Science* **281**, 269–272 (1998).
36. Nakanishi, J. *et al.* Imaging of conformational changes of proteins with a new environment- sensitive fluorescent probe designed for site-specific labeling of recombinant proteins in live cells. *Anal. Chem.* **73**, 2920–2928 (2001).
37. Adams, S. R. *et al.* New biarsenical ligands and tetracysteine motifs for protein labeling *in vitro* and *in vivo*: synthesis and biological applications. *J. Am. Chem. Soc.* **124**, 6063–6076 (2002).
38. Gaietta, G. *et al.* Multicolor and electron microscopic imaging of connexin trafficking. *Science* **296**, 503–507 (2002).
This paper describes the application of the tetracysteine–biarsenical system in pulse–chase labelling and electron microscopy.
39. Lauf, U. *et al.* Dynamic trafficking and delivery of connexons to the plasma membrane and accretion to gap junctions in living cells. *Proc. Natl Acad. Sci. USA* **99**, 10446–10451 (2002).
40. Farinas, J. & Verkman, A. S. Receptor-mediated targeting of fluorescent probes in living cells. *J. Biol. Chem.* **274**, 7603–7608 (1999).
41. Wu, M. M. *et al.* Organelle pH studies using targeted avidin and fluorescein-biotin. *Chem. Biol.* **7**, 197–209 (2000).
42. Wu, M. M. *et al.* Studying organelle physiology using targeted avidin and fluorescein-biotin. *Methods Enzymol.* **327**, 546–564 (2000).
43. Wu, M. M. *et al.* Mechanisms of pH regulation in the regulated secretory pathway. *J. Biol. Chem.* **276**, 33027–33035 (2001).
44. Sano, T. & Cantor, C. R. Expression of a cloned *streptavidin* gene in *Escherichia coli*. *Proc. Natl Acad. Sci. USA* **87**, 142–146 (1990).
45. Gambetta, G. A. & Lagarias, J. C. Genetic engineering of phytochrome biosynthesis in bacteria. *Proc. Natl Acad. Sci. USA* **98**, 10566–10571 (2001).
46. Tooley, A. J., Cai, Y. A. & Glazer, A. N. Biosynthesis of a fluorescent cyanobacterial C-phycocyanin holo-α subunit in a heterologous host. *Proc. Natl Acad. Sci. USA* **98**, 10560–10565 (2001).
47. Tooley, A. J. & Glazer, A. N. Biosynthesis of the cyanobacterial light-harvesting polypeptide phycoerythrocyanin holo-α subunit in a heterologous host. *J. Bacteriol.* **184**, 4666–4671 (2002).
48. Murphy, J. T. & Lagarias, J. C. The phytofluors: a new class of fluorescent protein probes. *Curr. Biol.* **7**, 870–876 (1997).
49. Wädt, S. & Deuschle, U. cobA, a red fluorescent transcriptional reporter for *Escherichia coli*, yeast, and mammalian cells. *Nature Biotechnol.* **17**, 1175–1178 (1999).
50. Cubitt, A. B. *et al.* Understanding, using and improving green fluorescent protein. *Trends Biochem. Sci.* **20**, 448–455 (1995).
51. Gonzalez, C. & Bejarano, L. A. Protein traps: using intracellular localization for cloning. *Trends Cell Biol.* **10**, 162–165 (2000).
52. Waterman-Storer, C. M., Desai, A., Bulinski, J. C. & Salmon, E. D. Fluorescent speckle microscopy, a method to visualize the dynamics of protein assemblies in living cells. *Curr. Biol.* **8**, 1227–1230 (1998).
53. Watanabe, N. & Mitchison, T. J. Single-molecule speckle analysis of actin filament turnover in lamellipodia. *Science* **295**, 1083–1086 (2002).
54. Bulinski, J. C., Odde, D. J., Howell, B. J., Salmon, T. D. & Waterman-Storer, C. M. Rapid dynamics of the microtubule binding of ensconsin *in vivo*. *J. Cell Sci.* **114**, 3885–3897 (2001).
55. Watton, S. J. & Downward, J. Akt/PKB localisation and 3′ phosphoinositide generation at sites of epithelial cell–matrix and cell–cell interaction. *Curr. Biol.* **9**, 433–436 (1999).
56. Oatey, P. B. *et al.* Confocal imaging of the subcellular distribution of phosphatidylinositol 3,4,5-trisphosphate in insulin- and PDGF-stimulated 3T3-L1 adipocytes. *Biochem. J.* **344**, 511–518 (1999).
57. Gray, A., Van Der, K. J. & Downes, C. P. The pleckstrin homology domains of protein kinase B and GRP1 (general receptor for phosphoinositides-1) are sensitive and selective probes for the cellular detection of phosphatidylinositol 3,4-bisphosphate and/or phosphatidylinositol 3,4,5-trisphosphate *in vivo*. *Biochem. J.* **344**, 929–936 (1999).
58. Servant, G. *et al.* Polarization of chemoattractant receptor signaling during neutrophil chemotaxis. *Science* **287**, 1037–1040 (2000).
59. Meili, R. *et al.* Chemoattractant-mediated transient activation and membrane localization of Akt/PKB is required for efficient chemotaxis to cAMP in *Dictyostelium*. *EMBO J.* **18**, 2092–2105 (1999).
60. Stauffer, T. P., Ahn, S. & Meyer, T. Receptor-induced transient reduction in plasma membrane $PtdIns(4,5)P_2$ concentration monitored in living cells. *Curr. Biol.* **8**, 343–346 (1998).
61. Hirose, K., Kadowaki, S., Tanabe, M., Takeshima, H. & Lino, M. Spatiotemporal dynamics of inositol 1,4,5-trisphosphate that underlies complex Ca^{2+} mobilization patterns. *Science* **284**, 1527–1530 (1999).
62. Oancea, E., Teruel, M. N., Quest, A. F. G. & Meyer, T. Green fluorescent protein (GFP)-tagged cysteine-rich domains from protein kinase C as fluorescent indicators for diacylglycerol signaling in living cells. *J. Cell Biol.* **140**, 485–498 (1998).
63. Teruel, M. N. & Meyer, T. Parallel single-cell monitoring of receptor-triggered membrane translocation of a calcium-sensing protein module. *Science* **295**, 1910–1912 (2002).
64. Oancea, E. & Meyer, T. Protein kinase C as a molecular machine for decoding calcium and diacylglycerol signals. *Cell* **95**, 307–318 (1998).
Reference 64 compares the kinetics of translocation of full-length PKC versus individual DAG-binding C1 domain and Ca^{2+}-binding C2 domain, which led to a model for a sequential activation of PKC through a temporal coordination between Ca^{2+} and DAG signals.
65. Ritzo, M. A., Shome, K., Watkins, S. C. & Romero, G. The recruitment of Raf-1 to membranes is mediated by direct interaction with phosphatidic acid and is independent of association with Ras. *J. Biol. Chem.* **275**, 23911–23918 (2000).
66. Dirks, R. W., Molenaar, C. & Tanke, H. J. Methods for visualizing RNA processing and transport pathways in living cells. *Histochem. Cell Biol.* **115**, 3–11 (2001).
67. Bassell, G. J., Oleynikov, Y. & Singer, R. H. The travels of mRNAs through all cells large and small. *FASEB J.* **13**, 447–454 (1999).
68. Bertrand, E. *et al.* Localization of ASH1 mRNA particles in living yeast. *Mol. Cell* **2**, 437–445 (1998).
69. Theurkauf, W. E. & Hazelrigg, T. I. *In vivo* analyses of cytoplasmic transport and cytoskeletal organization during *Drosophila* oogenesis: characterization of a multi-step anterior localization pathway. *Development* **125**, 3655–3666 (1998).
70. Zhang, H. L. *et al.* Neurotrophin-induced transport of a β-actin mRNP complex increases β-actin levels and stimulates growth cone motility. *Neuron* **31**, 261–275 (2001).
71. Muller, W. G., Walker, D., Hager, G. L. & McNally, J. G. Large-scale chromatin decondensation and recondensation regulated by transcription from a natural promoter. *J. Cell Biol.* **154**, 33–48 (2001).
72. Tsukamoto, T. *et al.* Visualization of gene activity in living cells. *Nature Cell Biol.* **2**, 871–878 (2000).
73. Straight, A. F., Marshall, W. F., Sedat, J. W. & Murray, A. W. Mitosis in living budding yeast: anaphase A but no metaphase plate. *Science* **277**, 574–578 (1997).
74. Robinett, C. C. *et al.* *In vivo* localization of DNA sequences and visualization of large-scale chromatin organization using lac operator/repressor recognition. *J. Cell Biol.* **135**, 1685–1700 (1996).
75. Hadjantonakis, A. K. & Nagy, A. The color of mice: in the light of GFP-variant reporters. *Histochem. Cell Biol.* **115**, 49–58 (2001).
76. Zlokarnik, G. *et al.* Quantitation of transcription and clonal selection of single living cells using β-lactamase as reporter. *Science* **279**, 84–88 (1998).
77. Li, X. *et al.* Generation of destabilized green fluorescent protein as a transcription reporter. *J. Biol. Chem.* **273**, 34970–34975 (1998).
78. Terskikh, A. *et al.* "Fluorescent timer": protein that changes color with time. *Science* **290**, 1585–1588 (2000).
This paper describes a DsRed-derived transcriptional reporter that changes colour from green to red over a period of 24 h, thereby preserving the temporal history of promoter activation.
79. Dantuma, N. P., Lindsten, K., Glas, R., Jellne, M. & Masucci, M. G. Short-lived green fluorescent proteins for quantifying ubiquitin/proteasome-dependent proteolysis in living cells. *Nature Biotechnol.* **18**, 538–543 (2000).
80. Kaether, C. & Gerdes, H. H. Visualization of protein transport along the secretory pathway using green fluorescent protein. *FEBS Lett.* **369**, 267–271 (1995).
81. Rudolf, R., Salm, T., Rustom, A. & Gerdes, H. H. Dynamics of immature secretory granules: role of cytoskeletal elements during transport, cortical restriction, and F-actin-dependent tethering. *Mol. Biol. Cell* **12**, 1353–1365 (2001).
82. Kneen, M., Farinas, J., Li, Y. & Verkman, A. S. Green fluorescent protein as a noninvasive intracellular pH indicator. *Biophys. J.* **74**, 1591–1599 (1998).
83. Llopis, J., McCaffery, J. M., Miyawaki, A., Farquhar, M. G. & Tsien, R. Y. Measurement of cytosolic, mitochondrial and Golgi pH in single living cells with green fluorescent protein. *Proc. Natl Acad. Sci. USA* **95**, 6803–6808 (1998).
84. Miesenböck, G., De Angelis, D. A. & Rothman, J. E. Visualizing secretion and synaptic transmission with pH-sensitive green fluorescent proteins. *Nature* **394**, 192–195 (1998).
Reference 84 describes 'synapto-pHluorins' that report synaptic neurotransmitter secretion by detecting the abrupt pH change that occurs when the acidic interior of the vesicle (pH ~5) is exposed to the outside of the cell (pH ~7) on fusion to the plasma membrane.
85. Matsuyama, S., Llopis, J., Deveraux, Q. L., Tsien, R. Y. & Reed, J. C. Changes in intramitochondrial and cytosolic pH: early events that modulate caspase activation during apoptosis. *Nature Cell Biol.* **2**, 318–325 (2000).
86. Wachter, R. M. & Remington, S. J. Sensitivity of the yellow variant of green fluorescent protein to halides and nitrate. *Curr. Biol.* **9**, R628–R629 (1999).
87. Wachter, R. M., Yarbrough, D., Kallio, K. & Remington, S. J. Crystallographic and energetic analysis of binding of selected anions to the yellow variants of green fluorescent protein. *J. Mol. Biol.* **301**, 157–171 (2000).
88. Jayaraman, S., Haggie, P., Wachter, R. M., Remington, S. J. & Verkman, A. S. Mechanism and cellular applications of a green fluorescent protein-based halide sensor. *J. Biol. Chem.* **275**, 6047–6050 (2000).
89. Elsliger, M.-A., Wachter, R. M., Hanson, G. T., Kallio, K. & Remington, S. J. Structural and spectral response of green fluorescent protein variants to changes in pH. *Biochemistry* **38**, 5296–5301 (1999).
90. Kuner, T. & Augustine, G. J. A genetically encoded ratiometric neurotechnique indicator for chloride: capturing chloride transients in cultured hippocampal neurons. *Neuron* **27**, 447–459 (2000).
91. Barondeau, D. P., Kassmann, C. J., Tainer, J. A. & Getzoff, E. D. Structural chemistry of a green fluorescent protein Zn biosensor. *J. Am. Chem. Soc.* **124**, 3522–3524 (2002).
92. Ostergaard, H., Henriksen, A., Hansen, F. G. & Winther, J. R. Shedding light on disulfide bond formation: engineering a redox switch in green fluorescent protein. *EMBO J.* **20**, 5853–5862 (2001).
93. Baird, G. S., Zacharias, D. A. & Tsien, R. Y. Circular permutation and receptor insertion within green fluorescent proteins. *Proc. Natl Acad. Sci. USA* **96**, 11241–11246 (1999).
94. Rapizzi, E. *et al.* Recombinant expression of the voltage-dependent anion channel enhances the transfer of Ca^{2+} microdomains to mitochondria. *J. Cell Biol.* (in the press).
95. Yu, D., Baird, G., Tsien, R. Y. & Davis, R. L. Detection of calcium transient in *Drosophila* mushroom body neurons with camgaroo. *J. Neurosci.* [in the press].
96. Siegel, M. S. & Isacoff, E. Y. A genetically encoded optical probe of membrane voltage. *Neuron* **19**, 735–741 (1997).
97. Ataka, K. & Pieribone, V. A. A genetically targetable fluorescent probe of channel gating with rapid kinetics. *Biophys. J.* **82**, 509–516 (2002).
98. Nakai, J., Ohkura, M. & Imoto, K. A high signal-to-noise Ca^{2+} probe composed of a single green fluorescent protein. *Nature Biotechnol.* **19**, 137–141 (2001).
99. Nagai, T., Sawano, A., Park, E. & Miyawaki, A. Circularly permuted green fluorescent proteins engineered to sense Ca^{2+}. *Proc. Natl Acad. Sci. USA* **98**, 3197–3202 (2001).
References 98 and 99 describe the insertion of circularly permuted GFP between calmodulin and M13 to yield Ca^{2+} indicators that have been dubbed 'GCaMP' and 'pericams', respectively.
100. Heim, R. & Tsien, R. Y. Engineering green fluorescent protein for improved brightness, longer wavelengths and fluorescence energy transfer. *Curr. Biol.* **6**, 178–182 (1996).
101. Mitra, R. D., Silva, C. M. & Youvan, D. C. Fluorescence resonance energy transfer between blue-emitting and red-shifted excitation derivatives of the green fluorescent protein. *Gene* **173**, 13–17 (1996).
102. Mahajan, N. P., Harrison-Shostak, D. C., Michaux, J. & Herman, B. Novel mutant green fluorescent protein protease substrates reveal the activation of specific caspases during apoptosis. *Chem. Biol.* **6**, 401–409 (1999).

103. Luo, K. Q., Yu, V. C., Pu, Y. & Chang, D. C. Application of the fluorescence resonance energy transfer method for studying the dynamics of caspase-3 activation during UV-induced apoptosis in living HeLa cells. *Biochem. Biophys. Res. Commun.* **283**, 1054–1060 (2001).
104. Rehm, M. *et al.* Single-cell fluorescence resonance energy transfer analysis demonstrates that caspase activation during apoptosis is a rapid process. Role of caspase-3. *J Biol. Chem.* **277**, 24506–24514 (2002).
105. Miyawaki, A. *et al.* Fluorescent indicators for Ca^{2+} based on green fluorescent proteins and calmodulin. *Nature* **388**, 882–887 (1997).
106. Miyawaki, A., Griesbeck, O., Heim, R. & Tsien, R. Y. Dynamic and quantitative Ca^{2+} measurements using improved cameleons. *Proc. Natl Acad. Sci. USA* **96**, 2135–2140 (1999).
107. Miyawaki, A. & Tsien, R. Y. Monitoring protein conformations and interactions by fluorescence resonance energy transfer between mutants of green fluorescent protein. *Methods Enzymol.* **327**, 472–500 (2000).
108. Truong, K. *et al.* FRET-based *in vivo* Ca^{2+} imaging by a new calmodulin-GFP fusion molecule. *Nature Struct. Biol.* **8**, 1069–1073 (2001).
109. Romoser, V. A., Hinkle, P. M. & Persechini, A. Detection in living cells of Ca^{2+}-dependent changes in the fluorescence emission of an indicator composed of two green fluorescent protein variants linked by a calmodulin-binding sequence. *J. Biol. Chem.* **272**, 13270–13274 (1997).
References 105 and 109 describe the first genetically encoded indicators to be composed of conformationally responsive elements sandwiched between two fluorescent proteins that can undergo FRET — a design that has since been extended to many other systems.
110. Persechini, A. & Cronk, B. The relationship between the free concentrations of Ca^{2+} and Ca^{2+}–calmodulin in intact cells. *J. Biol. Chem.* **274**, 6827–6830 (1999).
111. Sato, M., Hida, N., Ozawa, T. & Umezawa, Y. Fluorescent indicators for cyclic GMP based on cyclic GMP-dependent protein kinase Iα and green fluorescent proteins. *Anal. Chem.* **72**, 5918–5924 (2000).
112. Honda, A. *et al.* Spatiotemporal dynamics of guanosine 3′,5′-cyclic monophosphate revealed by a genetically encoded, fluorescent indicator. *Proc. Natl Acad. Sci. USA* **98**, 2437–2442 (2001).
113. Mochizuki, N. *et al.* Spatio-temporal images of growth-factor-induced activation of Ras and Rap1. *Nature* **411**, 1065–1068 (2001).
114. Kalab, P., Weis, K. & Heald, R. Visualization of a Ran-GTP gradient in interphase and mitotic *Xenopus* egg extracts. *Science* **295**, 2452–2456 (2002).
115. Kurokawa, K. *et al.* A pair of FRET-based probes for tyrosine phosphorylation of the Crkll adaptor protein *in vivo*. *J. Biol. Chem.* **276**, 31305–31310 (2001).
116. Ting, A. Y., Kain, K. H., Klemke, R. L. & Tsien, R. Y. Genetically encoded fluorescent reporters of protein tyrosine kinase activities in living cells. *Proc. Natl Acad. Sci. USA* **98**, 15003–15008 (2001).
117. Sato, M., Ozawa, T., Inukai, K., Asano, T. & Umezawa, Y. Fluorescent indicators for imaging protein phosphorylation in single living cells. *Nature Biotechnol.* **20**, 287–294 (2002).
118. Zhang, J., Ma, Y., Taylor, S. S. & Tsien, R. Y. Genetically encoded reporters of protein kinase A activity reveal impact of substrate tethering. *Proc. Natl Acad. Sci. USA* **98**, 14997–15002 (2001).
References 116 and 118 describe a general strategy for non-destructively imaging kinase activities in living cells using FRET-based reporters.
119. Sakai, R., Repunte-Canonigo, V., Raj, C. D. & Knoptel, T. Design and characterization of a DNA-encoded, voltage-sensitive fluorescent protein. *Eur. J. Neurosci.* **13**, 2314–2318 (2001).
120. Adams, S. R., Harootunian, A. T., Buechler, Y. J., Taylor, S. S. & Tsien, R. Y. Fluorescence ratio imaging of cyclic AMP in single cells. *Nature* **349**, 694–697 (1991).
121. Zaccolo, M. *et al.* A genetically encoded, fluorescent indicator for cyclic AMP in living cells. *Nature Cell Biol.* **2**, 25–29 (2000).
122. Zaccolo, M. & Pozzan, T. Discrete microdomains with high concentration of cAMP in stimulated rat neonatal cardiac myocytes. *Science* **295**, 1711–1715 (2002).
The use of a genetically encodable intermolecular FRET-based cAMP indicator in cardiac myocytes showed an unusual compartmentalization of cAMP.
123. Bacskai, B. J. *et al.* Spatially resolved dynamics of cAMP and protein kinase A subunits in *Aplysia* sensory neurons. *Science* **260**, 222–226 (1993).
124. Hempel, C. M., Vincent, P., Adams, S. R., Tsien, R. Y. & Selverston, A. I. Spatio-temporal dynamics of cAMP signals in an intact neural circuit. *Nature* **384**, 166–169 (1996).
125. Periasamy, A., Kay, S. A. & Day, R. N. in *Functional Imaging and Optical Manipulation of Living Cells*. SPIE Proc. Vol. 2983 (eds Farkas, D. L. & Tromberg, B. J.) (The International Society for Optical Engineers, USA, 1997).
126. Llopis, J. *et al.* Ligand-dependent interactions of coactivators SRC-1 and PBP with nuclear hormone receptors can be imaged in live cells and are required for transcription. *Proc. Natl Acad. Sci. USA* **97**, 4363–4368 (2000).
127. Janetopoulos, C., Jin, T. & Devreotes, P. Receptor-mediated activation of heterotrimeric G proteins in living cells. *Science* **291**, 2408–2411 (2001).
128. Damelin, M. & Silver, P. A. Mapping interactions between nuclear transport factors in living cells reveals pathways through the nuclear pore complex. *Mol. Cell* **5**, 133–140 (2000).
129. Ruehr, M. L., Zakhary, D. R., Damron, D. S. & Bond, M. Cyclic AMP-dependent protein kinase binding to A-kinase anchoring proteins in living cells by fluorescence resonance energy transfer of green fluorescent protein fusion proteins. *J. Biol. Chem.* **274**, 33092–33096 (1999).
130. Siegel, R. M. *et al.* Fas preassociation required for apoptosis signaling and dominant inhibition by pathogenic mutations. *Science* **288**, 2354–2357 (2000).
131. Xia, Z., Zhou, Q., Lin, J. & Liu, Y. Stable SNARE complex prior to evoked synaptic vesicle fusion revealed by fluorescence resonance energy transfer. *J. Biol. Chem.* **276**, 1766–1771 (2001).
132. Li, H. Y. *et al.* Protein–protein interaction of FHL3 with FHL2 and visualization of their interaction by green fluorescent proteins (GFP) two-fusion fluorescence resonance energy transfer (FRET). *J. Cell. Biochem.* **80**, 293–303 (2001).
133. Mas, P., Devlin, P. F., Panda, S. & Kay, S. A. Functional interaction of phytochrome B and cryptochrome 2. *Nature* **408**, 207–211 (2000).
134. Tertoolen, L. G. *et al.* Dimerization of receptor protein-tyrosine phosphatase α in living cells. *B.M.C. Cell Biol.* **2**, 8 (2001).
135. Ghosh, I., Hamilton, A. D. & Regan, L. Antiparallel leucine zipper-directed protein reassembly: Application to the green fluorescent protein. *J. Am. Chem. Soc.* **122**, 5658–5659 (2000).
136. Hu, C.-D., Chinenov, Y. & Kerppola, T. K. Visualization of interactions among bZIP and Rel family proteins in living cells using bimolecular fluorescence complementation. *Mol. Cell* **9**, 789–798 (2002).
137. Rossi, F., Charlton, C. A. & Blau, H. M. Monitoring protein-protein interactions in intact eukaryotic cells by β-galactosidase complementation. *Proc. Natl Acad. Sci. USA* **94**, 8405–8410 (1997).
138. Michnick, S. W., Remy, I., Campbell-Valois, F. X., Vallee-Belisle, A. & Pelletier, J. N. Detection of protein–protein interactions by protein fragment complementation strategies. *Methods Enzymol.* **328**, 208–230 (2000).
139. Wehrman, T., Kleaveland, B., Her, J. H., Balint, R. F. & Blau, H. M. Protein–protein interactions monitored in mammalian cells via complementation of β-lactamase enzyme fragments. *Proc. Natl Acad. Sci. USA* **99**, 3469–3474 (2002).
140. Galarneau, A., Primeau, M., Trudeau, L. E. & Michnick, S. W. β-Lactamase protein fragment complementation assays as *in vivo* and *in vitro* sensors of protein–protein interactions. *Nature Biotechnol.* **20**, 619–622 (2002).
141. Gordon, G. W., Berry, G., Liang, X. H., Levine, B. & Herman, B. Quantitative fluorescence resonance energy transfer measurements using fluorescence microscopy. *Biophys. J.* **74**, 2702–2713 (1998).
142. Sorkin, A., McClure, M., Huang, F. & Carter, R. Interaction of EGF receptor and grb2 in living cells visualized by fluorescence resonance energy transfer (FRET) microscopy. *Curr. Biol.* **10**, 1395–1398 (2000).
143. Erickson, M. G., Alseikhan, B. A., Peterson, B. Z. & Yue, D. T. Preassociation of calmodulin with voltage-gated Ca^{2+} channels revealed by FRET in single living cells. *Neuron* **31**, 973–985 (2001).
144. Chan, F. K. *et al.* Fluorescence resonance energy transfer analysis of cell surface receptor interactions and signaling using spectral variants of the green fluorescent protein. *Cytometry* **44**, 361–368 (2001).
145. Ng, T. *et al.* Imaging protein kinase Cα activation in cells. *Science* **283**, 2085–2089 (1999).
146. Verveer, P. J., Wouters, F. S., Reynolds, A. R. & Bastiaens, P. I. Quantitative imaging of lateral ErbB1 receptor signal propagation in the plasma membrane. *Science* **290**, 1567–1570 (2000).
147. Harpur, A. G., Wouters, F. S. & Bastiaens, P. I. Imaging FRET between spectrally similar GFP molecules in single cells. *Nature Biotechnol.* **19**, 167–169 (2001).
148. Weiss, S. Fluorescence spectroscopy of single biomolecules. *Science* **283**, 1676–1683 (1999).
149. Sako, Y., Minoguchi, S. & Yanagida, T. Single-molecule imaging of EGFR signalling on the surface of living cells. *Nature Cell Biol.* **2**, 168–172 (2000).
150. Sonnleitner, A., Mannuzzu, L. M., Terakawa, S. & Isacoff, E. Y. Structural rearrangements in single ion channels detected optically in living cells. *Proc. Natl Acad. Sci. USA* **99**, 12759–12764 (2002).
151. Harms, G. S. *et al.* Single-molecule imaging of l-type Ca^{2+} channels in live cells. *Biophys. J.* **81**, 2639–2646 (2001).
152. Ito, S. *et al.* Real-time observation of micrometastasis formation in the living mouse liver using a green fluorescent protein gene-tagged rat tongue carcinoma cell line. *Int. J. Cancer* **93**, 212–217 (2001).
153. Brown, E. B. *et al. In vivo* measurement of gene expression, angiogenesis and physiological function in tumors using multiphoton laser scanning microscopy. *Nature Med.* **7**, 864–868 (2001).

Acknowledgements

We thank S. R. Adams and J. Babendure for their comments on the manuscript. This work was supported by a National Institutes of Health grant to R.Y.T. and postdoctoral fellowship to A.Y.T, a grant from the Alliance for Cellular Signaling (to J.Z. and R.Y.T.) and the Howard Hughes Medical Institute. J.Z. is supported in part by a postdoctoral fellowship from La Jolla Interfaces in Science and Burroughs Wellcome Fund, and R.E.C. is supported in part by a postdoctoral fellowship from the Canadian Institutes of Health Research.

Online links

DATABASES

The following terms in this article are linked online to:
Entrez: http://www.ncbi.nlm.nih.gov/Entrez/
Kaede
Swiss-Prot: http://www.expasy.ch/
CFTR | EGF | GFP | ZBP

FURTHER INFORMATION

Roger Y. Tsien's laboratory:
http://www.tsienlab.ucsd.edu
Alice Y. Ting's laboratory:
http://web.mit.edu/chemistry/Ting_Lab/
BD Biosciences Clontech (EGFP, YFP–S65G/V68L/S72A/T203Y, CFP, DsRed2, HcRed, Fluorescent Timer, and DsRed-Express):
http://www.clontech.com
NanoLight Technology (*Renilla mulleri* GFP):
http://www.nanolight.com
PanVera (FlAsH–EDT$_2$ and ReAsH–EDT$_2$ labelling kits):
http://www.panvera.com
Access to this interactive links box is free online.